

**BULETINUL
INSTITUTULUI
POLITEHNIC
DIN IAȘI**

Tomul LVIII (LXII)

Fasc. 2

ȘTIINȚA ȘI INGINERIA MATERIALELOR

2012

Editura POLITEHNIUM

BULETINUL INSTITUTULUI POLITEHNIC DIN IAȘI
Published by the
„GHEORGHE ASACHI” TECHNICAL UNIVERSITY OF IAȘI
Editorial Office: Bd. D. Mangeron 63, 700050, Iași, ROMANIA
Tel. 40-232-278683; Fax: 40-232 237666; e-mail: polytech@mail.tuiasi.ro

Editorial Board

President: Prof. Dr. Eng. **Ion Giurma**,
Rector of the “Gheorghe Asachi” Technical University of Iași
Editor-in-Chief: Prof. Dr. Eng. **Carmen Teodosiu**,
Vice-Rector of the “Gheorghe Asachi” Technical University of Iași
Honorary Editors: Prof. Dr. Eng. **Alfred Braier**,
Prof. Dr. Eng. **Hugo Rosman**

Editorial Staff of the Section
MATERIALS SCIENCE AND ENGINEERING

Editors: Assoc. Prof. Dr. Eng. **Iulian Ioniță**
Assoc. Prof. Dr. Eng. **Gheorghe Bădărău**
Prof. Dr. Eng. **Dan Gelu Gălușcă**
Prof. Dr. Eng. **Costică Bejinariu**

Honorary Editors: Prof. Dr. Eng. **Ion Hopulele**, Prof. Dr. Eng. **Ion Mălureanu**,
Prof. Dr. Eng. **Adrian Dima**

Associated Editor: Assoc. Prof. Dr. Eng. **Ioan Rusu**

Editorial Advisory Board

Prof.dr.eng. Agustin Santana Lopez , La Palmas de Gran Canaria University, (Spain)	Assoc. Prof. Shizutoshi Ando , Tokyo University of Sciences, (Japan)
Prof.dr.eng. Mihai Susan , “Gheorghe Asachi” Technical University of Iași, (Romania)	Prof.dr.eng. Leandru-Gheorghe Bujoreanu , “Gheorghe Asachi” Technical University of Iași, (Romania)
Prof.dr.eng. Ioan Carcea , “Gheorghe Asachi” Technical University of Iași, (Romania)	Prof. dr. eng. Constantin Baci , “Gheorghe Asachi” Technical University of Iași, (Romania)
Prof.dr. Duu-Jong Lee , National Taiwan University of Science and Technology, (Taiwan)	Dr. Koichi Tsuchiya , National Institute for Materials Science (Japan)
Prof.dr.eng. Shih-Hsuan Chiu , National Taiwan University of Science and Technology, (Taiwan)	Dr.eng. Burak Özkal , Istanbul Technical University (Turkey)
Prof.dr.eng. Yuri A. Burennikov , Vinnitsya National Technical University, (Ukraine)	Prof. dr. eng. Vasile Cojocaru-Filipiuc , “Gheorghe Asachi” Technical University of Iași, (Romania)
Prof. dr. Oronzio Manca , Seconda Università degli Studi di Napoli (Italy)	Prof. dr. Viorel Păun , University “Politehnica” Bucharest, (Romania)
Prof.dr.eng. Julia Mirza Rosca , La Palmas de Gran Canaria University, (Spain)	Prof.dr. Maricel Agop , “Gheorghe Asachi” Technical University of Iași, (Romania)
Prof.dr.eng. Petrică Vizureanu , “Gheorghe Asachi” Technical University of Iași, (Romania)	Prof.dr.eng. Sergiu Stanciu , “Gheorghe Asachi” Technical University of Iași, (Romania)

ȘTIINȚA ȘI INGINERIA MATERIALELOR

SUMAR

	<u>Pag.</u>
GELU BARBU și ADRIAN ALEXANDRU, Influența vibrațiilor asupra durității aliajului Al-Cu-Si turnat (engl. rez. rom.)	9
MARIUS-GABRIEL SURU, ADRIAN-LIVIU PARASCHIV și LEANDRU-GHEORGHE BUJOREANU, Aspecte microstructurale noi ale plăcilor de martensită în aliajele cu memoria formei pe bază de Fe-Mn-Si și Cu-Zn-Al (engl. rez. rom.)	15
MIHAELA RĂȚOI, SERGIU STANCIU și ROMEU CHELARIU, Biomateriale pe bază de Fe pentru stenturi coronariene degradabile (engl. rez. rom.)	23
ELENA-RALUCA BACIU, IRINA GRĂDINARU, MARIA BACIU și NORINA CONSUELA FORNA, Considerații privind caracteristicile structurale și proprietățile aliajelor dentare cu baza titan (engl. rez. rom.)	35
CONSTANTIN CORĂBIERU, DAN DRAGOȘ VASILESCU, ANIȘOARA CORĂBIERU și PETRICĂ CORĂBIERU, Bimetale oțel – bronz obținute prin imersie și centrifugare verticală (engl. rez. rom.)	43
ANDREI VICTOR SANDU, COSTICĂ BEJINARIU, IOAN GABRIEL SANDU și CONSTANTIN BACIU, Studiu tribologic asupra unor straturi subțiri de fosfați de zinc (engl. rez. rom.)	51
V. SAVULIAK, A. YANCHENKO, A. POSTUPAILO și T. YAROSHENKO, Realizarea durificării compozitelor în aliajele bogate în carbon prin aliere cu elemente tensioactive (engl. rez. rom.)	57

MATERIALS SCIENCE AND ENGINEERING

CONTENTS

	<u>Pp.</u>
GELU BARBU and ADRIAN ALEXANDRU, The Influence of Vibrations upon Hardness at Al-Cu-Si Alloy Casting (English, Romanian summary)	9
MARIUS-GABRIEL SURU, ADRIAN-LIVIU PARASCHIV and LEANDRU-GHEORGHE BUJOREANU, Novel Micro Structural Aspects of Martensite Plates in Shape Memory Alloys Based on Fe-Mn-Si and Cu-Zn-Al (English, Romanian summary)	15
MIHAELA RĂȚOI, SERGIU STANCIU and ROMEU CHELARIU, Fe Basis Biomaterials for Degradable Coronary Stents (English, Romanian summary)	23
ELENA-RALUCA BACIU, IRINA GRĂDINARU, MARIA BACIU and NORINA CONSUELA FORNA, Considerations Regarding Structural Characteristics and Properties of Titanium Based Dental Alloys (English, Romanian summary)	35
CONSTANTIN CORĂBIERU, DAN DRAGOȘ VASILESCU, ANIȘOARA CORĂBIERU and PETRICĂ CORĂBIERU, Steel – Bronze Bimetal by Immersion and Vertical Centrifugation (English, Romanian summary)	43
ANDREI VICTOR SANDU, COSTICĂ BEJINARIU, IOAN GABRIEL SANDU and CONSTANTIN BACIU, Tribological Study on Some thin Zinc Phosphate Layers (English, Romanian summary)	51
V. SAVULIAK, A. YANCHENKO, A. POSTUPAILO and T. YAROSHENKO, Realization of Composite Hardening in High Carbonaceous Alloys by Alloying with Tensoactive Elements (English, Romanian summary)	57

BULETINUL INSTITUTULUI POLITEHNIC DIN IAȘI
Publicat de
Universitatea Tehnică „Gheorghe Asachi” din Iași
Tomul LVIII (LXII), Fasc. 2, 2012
Secția
ȘTIINȚA ȘI INGINERIA MATERIALELOR

THE INFLUENCE OF VIBRATIONS UPON HARDNESS AT Al-Cu-Si ALLOY CASTING

BY

GELU BARBU* and **ADRIAN ALEXANDRU**

“Gheorghe Asachi” Technical University of Iași
Faculty of Material Science and Engineering

Received: February 28, 2012

Accepted for publication: March 19, 2012

Abstract: The alloy which contains 90.1% Al, 5.16% Si, 2.09 Cu is vibrated circular-horizontally using an original vibrating system, studying the variation of hardness on longitudinal and transversal direction at some samples casted in shape of moulding sand and in metallic mould. The fact that bigger differences between the values of hardness at the samples casted under the influence of vibrations and the ones statically casted appears at the extremities of the pieces, when casted in moulding sand, and when the pieces were casted in metallic moulds, the bigger hardness differences are at the middle of the pieces, on horizontally direction. In all the cases the samples casted under the influence of vibrations have higher values of hardness than the ones statically casted.

Keywords: casting in vibration field; hardness; Al-Cu-Si alloy.

1. General Considerations

The obtaining processes of moulding parts are simple but they have some disadvantages such as chemical non-uniformity and structural non-uniformity which unfavorable influence the exploitation characteristics of products. Today efforts are made to find new technological solutions that could

* Corresponding author: *e-mail*: barbugelu1234@yahoo.com

bring, for the first time, the possibility of raising the capacity and finishing the structure of molded alloys.

Vibration is the motion of the particles of an elastic body or medium in alternately opposite directions from the position of equilibrium, periodically in time.

When vibrations are applied, a series of physical processes appear, like the action of count forces, the mass macroscopic transfer, cavitation phenomena, the amplification of the overcooling degree and changing of the conditions of solid-fluid equilibrium. Thus, shearing forces occur, which act on the growing dendrites, at the solid-fluid severance limit. The macroscopically mass transfer depends on the correlation between the amplitude and the frequency of the movement, the crystals which belong to the moving fluid will come into collision with the branch of the dendrites in the bracket, resulting a breaking effort.

The displacement of the alloy accomplishes in flowing regime given by the Reynolds criterion, in the expression interfering the amplitude and the casting frequency. When the relative speed between the fluid and the crystals is bigger than a critical speed, the cavitation phenomenon appears.

In bases of taken tests, a lot of written research proves that the maximum effect of vibration is in the same time of molding, in the formation period of crystallization germs.

The most important effects of vibrations applied on alloy molding are the higher homogeneity of the parts by decreasing the volume of microretats, improving the flow capacity, decreasing the gases contents, decreasing the segregation by stopping the continuum of displacing streams of the liquid enriched with elements that segregates.

The primary parameters of vibration are frequency, amplitude, vibration time, vibration type, parameters which can be optimized by the special conditions that appear on molding process.

The vibrations can be delivered to the metallic alloys by using the mechanical, electrical, hydraulic, pneumatic vibrators and by using ultrasonic and magnetic fields.

The vibrating source is assured by an eccentric trained by an electric engine, which can likely regulate the frequency and the amplitude.

2. Experiments

Attempts have been made to study the influence of the cooling speed and the vibrations applied to the aluminum solidification. Thereby shapes have been casted in molding sand and in metallic moulds, static and under the influence of the vibrations.

The chemical composition of the casted shapes is presented in Table 1.

For melting there has been used an electric furnace, with resistances, using pure metals, prealloys and alloy anterior melted, the liquid bath being protected with a layer of agent of fusion.

The casting temperature was 700°C, and the shapes have been preheated at a temperature of aprox. 100°C.

There have been casted control cylinders, in section, which were coped, and in the section were determined the values of hardness, according to Fig. 1, the results of the determinations being comprised in Tables 2,...,5.

Metallic forms were made of steel with a rectangular section. To check the influence of the cooling rate, metallic forms and forms made of molding sand were used.

Two castings were made:

a) the first was poured under static conditions, both for the mixture of the training form and shape metal;

b) the second batch was poured in dynamic conditions, both for the mixture of the training form and shape metal.

Samples were subjected to circular-horizontal vibrations during the solidification.

Table 1
Chemical Compositions of Casted Samples

Al	Cu	Mg	Si	Mn	Ni	Zn	Pb	Sn
90.1	2.09	1.33	5.16	0.9	0.15	1.40	0.29	0.81

Casted samples were marked: 1 – sample casted in mouldings sand, static; 2 – sample casted in mouldings sand, dynamic conditions; 3 – sample casted in metallic moulds, dynamic conditions; 4 – sample casted in metallic moulds, static.

Fig. 1 shows the position of points in the longitudinal section; hardness was measured.

	a	b	c	d	e	f
1
2
3
4
5
6

Fig. 1 – Position points in the longitudinal section - hardness was measured.

Hardness values for samples casted are included in Tables 2,..., 5.

Table 2
Hardness Values for Sample 1

	<i>a</i>	<i>b</i>	<i>c</i>	<i>d</i>	<i>e</i>	<i>f</i>	Media
<i>1</i>	75.4	68.1	75.3	69.2	67.3	70.3	70.93
<i>2</i>	73.5	69.2	76.1	67.2	60.4	70.8	68.22
<i>3</i>	67	73.7	63.8	75.2	59.6	68	67.88
<i>4</i>	71.5	74.3	73.3	78	72.7	78.2	74.67
<i>5</i>	73.3	66	66.7	67.5	75.8	71.1	70.07
<i>6</i>	59.9	72.2	70	76.6	71.9	74.3	70.82
Media	70.10	70.58	69.82	72.28	67.95	72.12	70.48

Table 3
Hardness Values for Sample 2

	<i>a</i>	<i>b</i>	<i>c</i>	<i>d</i>	<i>e</i>	<i>f</i>	Media
<i>1</i>	72.1	71.5	72.5	74.2	73.3	74.3	72.98
<i>2</i>	77.4	74.2	74.2	72.3	69.8	76.1	74.00
<i>3</i>	72.6	72.8	70.8	72	69.9	66.6	70.78
<i>4</i>	73.3	72.2	67	71.1	64.9	67.9	69.40
<i>5</i>	75.8	71.3	65.7	73.1	72.9	72.2	71.83
<i>6</i>	73.4	66	70	72.3	74.1	72.1	71.32
Media	74.10	71.33	70.03	72.50	70.82	71.53	71.72

Table 4
Hardness Values for Sample 3

	<i>a</i>	<i>b</i>	<i>c</i>	<i>d</i>	<i>e</i>	<i>f</i>	Media
<i>1</i>	74.1	73.5	72.4	76.2	74.3	75.2	74.28
<i>2</i>	77.4	75.1	76.2	71.3	70.8	76.3	74.52
<i>3</i>	72.8	74.8	71.7	73	69.8	70.6	72.12
<i>4</i>	73.2	72.5	70	70.1	69.8	68.9	70.75
<i>5</i>	75.8	70.3	73.7	73.4	72.8	73.2	73.20
<i>6</i>	73.4	69.9	70.7	72.53	74.7	73.1	72.39
Media	74.45	72.68	72.45	72.76	72.03	72.88	72.88

Table 5
Hardness Values for Sample 4

	<i>a</i>	<i>b</i>	<i>c</i>	<i>d</i>	<i>e</i>	<i>f</i>	Media
<i>1</i>	75.4	68.7	76.3	69.2	67.3	70.3	71.20
<i>2</i>	73.5	70.2	76.1	67.2	60.4	70.8	69.70
<i>3</i>	68.5	73.7	68.8	76.2	59.6	68	69.13
<i>4</i>	71.5	74.3	73.3	78	72.7	78.2	74.67
<i>5</i>	74.3	67.1	65.7	67.5	75.8	74.1	70.75
<i>6</i>	68.8	72.2	70.6	76.7	72.7	73.3	72.38
Media	72.00	71.03	71.80	72.47	68.08	72.45	71.31

Variation of hardness on section evidence is presented in the form of spatial graphs in Figs. 2,..., 5.

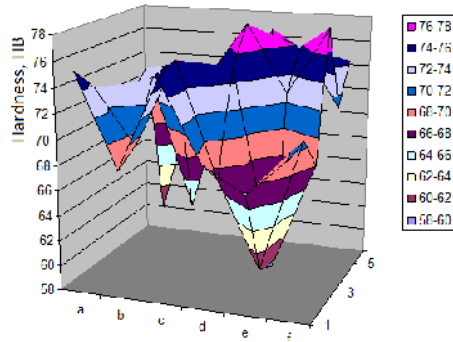


Fig. 2 – Variation of hardness test in section 1 (static cast in forms of moulding sand).

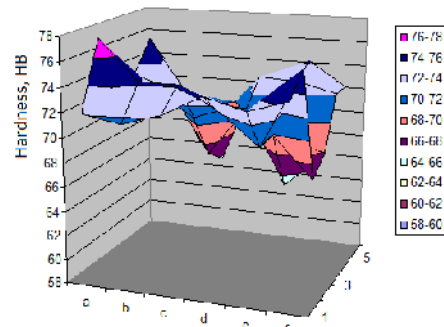


Fig. 3 – Variation of hardness proof in Section 2 (under the influence of vibrations, in moulding sand).

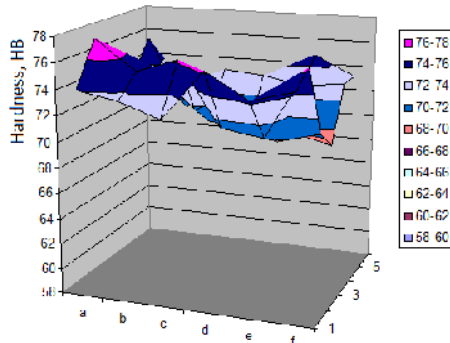


Fig. 4 – Variation of hardness in sample 3 (under the influence of vibration; metallic forms).

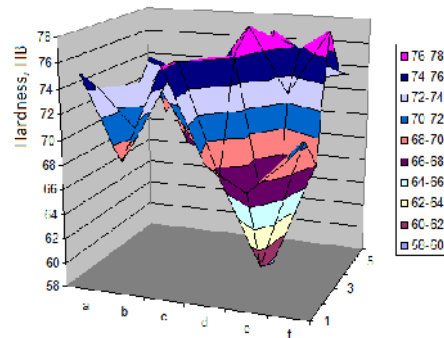


Fig. 5 – Variation of hardness in Section 3 (static casted in metallic forms).

3. Conclusions

Among the technological effects of the application of vibrations at solidification: the homogenization and the finishing of the solidification structure, the amplification of the compactification of the casted material, the degassing of the alloy, the shrinking of the segregations, the expulsion of non-metallic inclusions and the increase of the capacity of yielding alloy.

Bigger differences between the values of hardness at the shapes casted under the influence of the vibrations and the ones statically casted appear at the extremities of the pieces, when casting in shapes of moulding sand.

When the pieces are casted in metallic moulds the bigger differences of hardness are at the middle of the pieces, on horizontally course.

In all the cases the pieces casted in metallic shapes have bigger hardnesses than the ones statically casted.

There is an increasing evidence of medium hardness values in vibrated samples relative to the samples in static conditions, Table 6.

Table 6
Average Hardness Values of Casted Samples

Sample	Terms of casting	Hardness test HB
1	Moulding sand, static	70.65
2	Moulding sand, dynamic conditions	71.72
3	Metallic forms, dynamic conditions	72.88
4	Metallic forms, static	71.31

Increased density in the central and exterior cast part. This effect of vibrations occurs due to decrease of gas content, and high finishing structure. Positive effects of vibrations can be seen in Figs. 2,...,5; hardness values are more uniform throughout the whole section specimens.

REFERENCES

- Barbu G., *Solidificarea aliajelor sub influența vibrațiilor*. Edit. Vasiliana, Iași, 2003.
 Buzdugan Gh., *Vibrațiile sistemelor mecanice*. Edit. Academiei, București, 1970.
 Darie S., *Vibratoare electrice*. Edit. Tehnică, București, 1987.
 Dittmann O. et al., *Verfahren zur Herstellung von Barren aus Ferro-Legierungen, Kupfer-Legierungen, Aluminium-Legierungen und der gleichen*. Anmelder: Umemura, Ikuo, Tokio, Bundesrepublik Deutschland, Deutsches Patentamt, nr. 2.334.544, 06.06.1973.
 Ștefănescu Fl., Bratu C., *Cercetări privind influența vibrației asupra compactității aliajelor turnate*. Metalurgia, 5, 1985.
 Ștefănescu Fl., *Procese fizice care au loc la vibrarea aliajelor turnate. Efecte tehnologice. Principii de proiectare a instalațiilor de turnare*. Metalurgia, 9, 1987.

INFLUENȚA VIBRAȚIILOR ASUPRA DURITĂȚII ALIAJULUI Al-Cu-Si TURNAT

(Rezumat)

Aliajul care conține 91.1% Al, 4.85% Si, 2.32 Cu a fost vibrat circular orizontal cu un sistem original de vibrare, studiindu-se variația durității de direcție longitudinal și transversal la o serie de epruvete turnate în amestec de formare și în forme metalice. Cele mai mari diferențe între valorile durității la probele statice față de cele vibrare apar la extremități în cazul pieselor turnate în forme din amestec și în partea centrală când piesele sunt turnate în forme metalice. În toate cazurile epruvetele turnate sub influența vibrațiilor au duritate mai mare decât cele turnate static.

BULETINUL INSTITUTULUI POLITEHNIC DIN IAȘI
Publicat de
Universitatea Tehnică „Gheorghe Asachi” din Iași
Tomul LVIII (LXII), Fasc. 2, 2012
Secția
ȘTIINȚA ȘI INGINERIA MATERIALELOR

NOVEL MICRO STRUCTURAL ASPECTS OF MARTENSITE PLATES IN SHAPE MEMORY ALLOYS BASED ON Fe-Mn-Si AND Cu-Zn-Al

BY

MARIUS-GABRIEL SURU*, ADRIAN-LIVIU PARASCHIV
and LEANDRU-GHEORGHE BUJOREANU

“Gheorghe Asachi” Technical University of Iași
Faculty of Material Science and Engineering

Received: February 28, 2012

Accepted for publication: March 19, 2012

Abstract: New aspects of martensite plates of two shape memory alloys (SMAs) based on Fe–Mn–Si–Cr–Ni and Cu–Zn–Al, respectively, were analyzed from micro-structural point of view by scanning electron microscopy (SEM). Structural evaluations revealed larger dimensions of the plates of ϵ hexagonal close packed (hcp) martensite, in an Fe–Mn–Si–Cr–Ni SMA than those of $\beta 2'$ orthorhombic (9R) martensite, in a Cu–Zn–Al SMA. The 3D analyses were performed in order to emphasize the aspects of the width and height of plates, of both ϵ hcp $\beta 2'$ 9R martensites. For the observation of micro-structural aspects of both alloy systems, SEM micrographs were made as well as 3-D general micrographs.

Keywords: Fe-Mn-Si shape memory alloy; Cu-Zn-Al shape memory alloy; Martensite-plates, SEM.

1. Introduction

The Fe–Mn–Si alloys are known to exhibit an excellent shape memory effect and have been the subject of many efforts to develop low cost shape

* Corresponding author: *e-mail*: marius_suru2005@yahoo.com

memory materials. Much of this effort has been directed to the improvement of the corrosion resistance of these alloys, leading to the development of Fe–Mn–Si–Cr–Ni alloys and of similar alloys containing also Co (Sato *et al.*, 1982; Sato *et al.*, 1986).

Various parameters, such as alloy composition, applied stress, prestrain, grain size, pre-existing martensite and thermal cycling, influence the shape memory effect in Fe–Mn–Si alloys, as summarized by Gu *et al.* (1994).

Commercial shape memory alloys (SMAs) include Cu-Zn-Al base alloy, characterized by recovery strains and stresses as large as 4% and 400 MPa, respectively (Huang, 2002).

The main drawback in exploiting Cu-Zn-Al base SMAs, as functional materials, is diffusion-controlled martensite stabilization, occurring during successive heating even in low temperature range (Li *et al.*, 2008) and causing the shift of the critical temperatures for reverse martensitic transformation (A_s and A_f) to higher temperatures (Wang *et al.*, 2004).

Martensite was initially found as a hard structure component in quenched steels. If steel, in a high-temperature austenitic phase, is quenched it will generally harden. After polishing and etching, observations with a microscope will show an extremely fine structure, which was first named “martensite” after the eminent German metallurgist Adolf Martens. It was later shown that this structure resulted from a lattice transformation without atomic diffusion. The face-centred cubic (fcc) austenite transformed into lens-shaped or plate-like regions with body-centred cubic lattices or body-centred tetragonal lattices. The crystals created by such transformations are called “martensite” and lattice transformations without atomic diffusion are called “martensitic” transformations. Martensitic transformations are thus diffusionless transformations occurring in the solid state of materials (Delaey, 1995).

In alloys containing Cr and Ni, such as first the system based on Fe–Mn–Si–Cr–Ni, the strain induced γ (fcc) to ϵ (hcp) martensitic transformation is often accompanied by the γ to α' % (bcc) or ϵ to α' % transformations (Sato *et al.*, 1977). The majority of the studies concerning the influence of straining on the microstructure and properties of these alloys consider only small deformation in tension, compression or bending.

In the case of a martensitic Cu-Zn-Al SMA subjected to thermal cycling with free-air cooling, thermal memory degradation was associated with an alteration of martensite reversion to parent phase (Bujoreanu *et al.*, 2011). During cooling, β -type austenite undergoes an ordering reaction, from disordered β (A2) into ordered β_1 (L21) or β_2 (B2) from which β_3' (18R-monoclinic) or β_2' (9R orthorhombic) martensite, respectively, are thermally or stress induced (Ahlers, 1986).

This paper aims to present new micro structural aspects for these two systems of shape memory alloys (SMAs) based on Fe–Mn–Si–Cr–Ni and Cu-Zn-Al, respectively.

2. Experimental Procedure

A Fe–Mn–Si–Cr–Ni SMA was cast, homogenized, hot rolled (1,373 K), annealed and quenched (1,273 K/ 0.6 ks/ water). The chemical composition, determined by spectrogravimetry was 15.75Mn–12.26Cr–3.75Si–4.69Ni–0.42Mo–0.28Cu–0.065C–0.06V–0.04Co – 0.021S–0.019P balance Fe. From annealed raw material, tensile specimens with gauge dimensions $(1 \times 4 \times 20) \cdot 10^{-3}$ m were cut by spark erosion. After that the sample was subjected at 10 cycles of constrained recovery by means of an INSTRON 3382 tensile testing machine at room temperature (RT) (Bujoreanu, 2008). A 14,86Cu–5,81Zn–0,5Al–Fe SMA was cast, hot rolled, instant-water quenched and homogenized (1070K/ 18 ks/ water). These specimens were used for scanning electron microscopy (SEM) analysis, after they being cut, embedded, ground, electro-polished and etched (Bujoreanu *et al.*, 2008).

Scanning electron microscopy (SEM) observations were carried on a FEI Quanta SEM-FIB 200 3-D dual beam microscope, under protective atmosphere. By means of Quanta software, 3-D images were performed recorded, which have been used to emphasize the new aspects of the width and height of martensites plates from both systems of alloys.

3. Experimental Results and Discussion

SEM images of the microstructure of a specimen of Fe–Mn–Si–Cr–Ni SMA are shown in Fig. 1. Fig. 1 *a* displays a general aspect of ϵ hcp stress induced martensites plates, while Fig. 1 *b* illustrates a magnified detail of such a plate group.

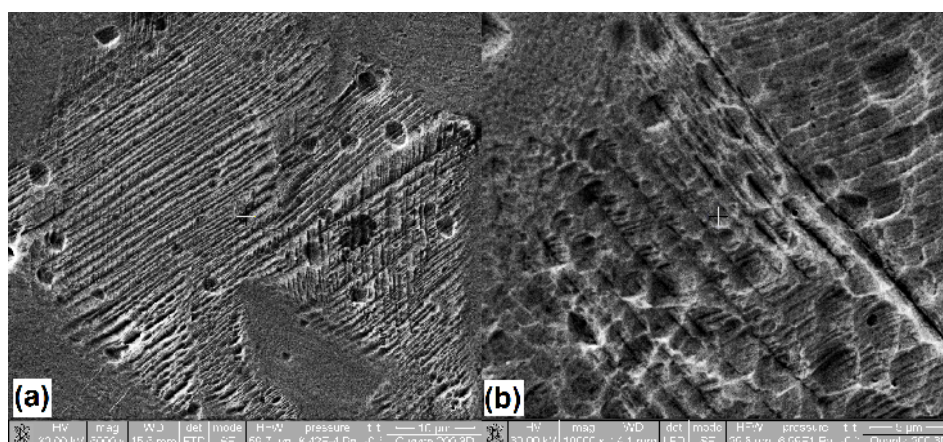


Fig. 1 – Micro-structural observation of martensite plates on SEM micrographs in Fe–Mn–Si–Cr–Ni SMA: *a* – general aspect of ϵ hcp martensite; *b* – detail of a plate group.

3-D evaluations were made on micrographs from Fig. 1 by mean of Quanta software. These images of 3-D evaluations are illustrated in Fig. 2. In this case, we observed that the widths and heights of stress induced martensite plates are larger in Fig. 2 *a*, corresponding to primary plates, than in Fig. 2 *b*, corresponding to secondary plates.

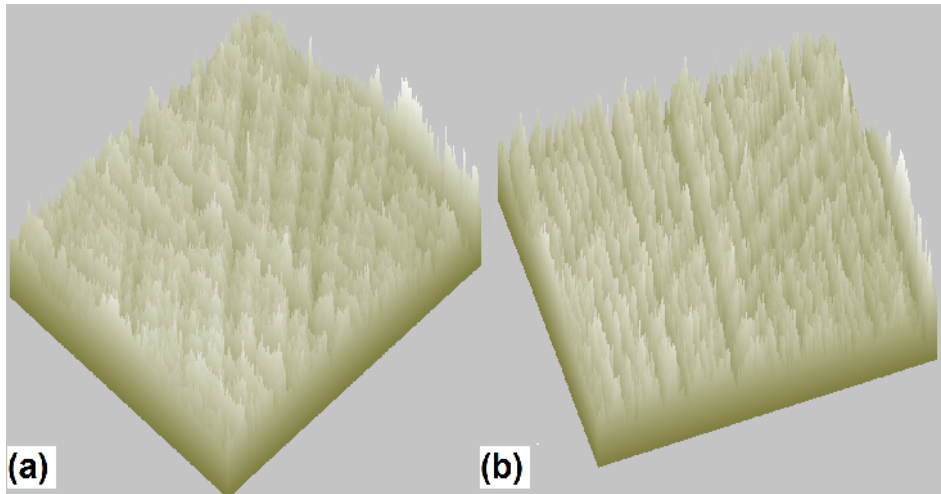


Fig. 2 – 3-D evaluation of martensite plates in Fe-Mn-Si-Cr-Ni SMA: *a* – primary plates; *b* – secondary plates.

From the 3-D details of the plate groups of ϵ hcp martensite in Fig. 2 we can say that the plates are quite smooth but can even specify that they contain sub-plates. As we mention that their depth is quite remarkable. The martensite plates, with typical thickness of the order of micrometers, have orientation in one single direction (Lohan *et al.*, 2010).

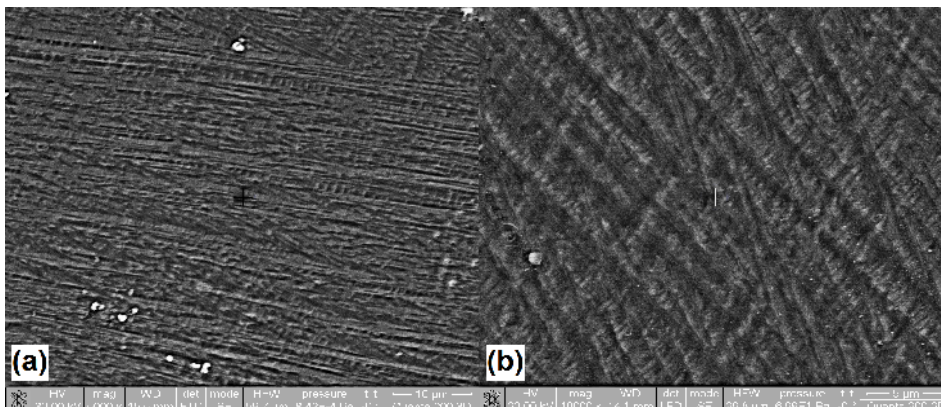


Fig.3 – Micro-structural observation of martensite plates on SEM micrographs of Cu-Zn-Al SMA: *a* – general aspect of β_2' 9R martensite; *b* – detail of a plate group.

SEM images of the microstructure of Cu-Zn-Al SMA specimen are shown in Fig. 3. This micrograph emphasizes in Fig. 3 *a* a general aspect of β_2' 9R thermally induced martensite plates, while Fig. 3 *b* illustrates a magnified detail of a plate group.

We note in this micrograph, two important facts: (i) the arrangement and orientation of the plates is very different from those of ϵ hcp, of course because this is thermally induced martensite, and (ii) the sub-plates are much clearer even in general aspect from Fig. 3 *a* but especially from Fig. 3 *b* in the detail of the plate group. From the general aspect of Cu-Zn-Al martensite we can specify that the orientation of the primary thermally induced martensite plates is different because they are developed according to several directions.

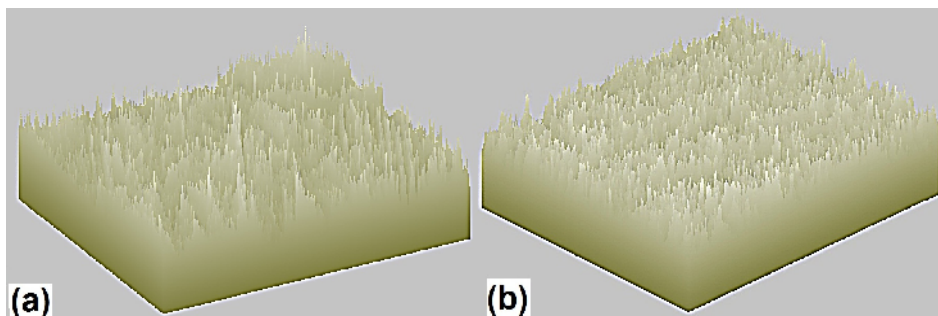


Fig.4 – 3-D evaluation of β_2' 9R martensite plates in Cu-Zn-Al SMA:
a – primary plates; *b* – secondary plates.

3-D evaluations were made on micrographs from Fig. 3 by mean of the same Quanta software. These images of 3-D evaluations are illustrated in Fig.4. From the 3-D evaluation of martensite plates of Cu-Zn-Al SMA in Fig. 4 we can say, at first sight, that the plates are thinner, as compared to those observed in Fe-Mn-Si-Cr-Ni, and evaluated in Fig. 2.

Moreover, we observed from Fig. 4 *b* that the secondary plates are much finer than those observed in Fe-Mn-Si-Cr-Ni.

On the 3-D evaluation of Fig. 4 *b* the widths and heights of martensite plates are more obvious and for this reason, the difference between primary and secondary plates is more noticeable in Cu-Zn-Al than in Fe-Mn-Si-Cr-Ni.

The detail of plate group reveals in Fig. 4 *b* that the plates of β_2' 9R martensite in Cu-Zn-Al SMA are not very deep, but we can say that they have a considerable height.

The sub-plates are visible on the 3-D evaluation and we can indicate that their presence plays an important role in shape memory phenomena.

4. Conclusions

Novel micro-structural aspects of martensites plates in shape memory alloys were revealed in the case of a Cu–15 Zn–6 Al SMA and an Fe–15.8 Mn–3.8 Si–12.3 Cr–4.7 Ni (mass. %) SMA.

SEM general observations have emphasized the different arrangement and orientation of the martensite plates in the case of the two analyzed systems of shape memory alloys. So we can say that the ϵ hcp stress induced martensites plates have orientation in one single direction, while the β_2' 9R thermally induced martensites plates have multiple orientations.

SEM micrographs made in detail of a plate group on each of the two alloy systems showed the presence of the sub-plates which are different for the two shape memory alloys.

From 3-D evaluation of martensite plates in Cu–Zn–Al, we can say at a first view that the plates are thinner than those of ϵ hcp stress induced in Fe–Mn–Si–Cr–Ni SMA and, the detail of plate group reveals that the plates of β_2' 9R Cu–Zn–Al shape memory alloy are not as deep as the plates from ϵ hcp Fe–Mn–Si–Cr–Ni shape memory alloy.

The β_2' 9R martensites plates seem not to be so smooth, large and deep as compared to ϵ hcp martensites plates.

REFERENCES

- Sato A., Chishima E., Soma K., Mori T., *Acta Metall*, **30**, 1177 (1982).
Sato A., Yamaji Y., Mori T., *Acta Metall*, **34**, 287 (1986).
Gu Q., Van Humbeeck J., Delaey L., *J. Phys., France*, **IV 4 C3–135**. 627 (1994).
Huang W., *Mater Design*, **23**, 11 (2002).
Li Z., Gong S., Wang M. P., *J Alloy Compd.*, **452**, 307 (2008).
Wang Z.G., Zu X.T., Wu J.H., Liu L.J., Mo H.Q., Huo Y., *J Alloy Compd.*, **364**, 171 (2004).
Delaey L., Chapter 6 in *Materials Science and Technology*, Voi. 5: Phase Transformations in Materials, Ed. R.W. Cahn, P. Haasen, E.J. Kramer, VCH, Weinheim, (1995).
Sato A., Sunaga Y., Mori T., *Acta Metall.*, **25** (1977).
Bujoreanu L.G., Lohan N.M., Pricop B., Cimpoesu N., *J. Mater. Eng. Perform.*, **20**, 468 (2011).
Ahlers M., *Prog. Mater. Sci.*, **135** (1986).
Bujoreanu L.G., Stanciu S., Comaneci R.I., Meyer M., Dia V., Lohan C., *JMEPEG*, **500–505** (2009).
Bujoreanu L.G., *Mat. Sci. Eng., A*, **481–482**, (2008).
Bujoreanu L.G. *et al.*, *Eur. Phys. J. Special Topics*, **158**, 15 (2008).
Lohan C., Pricop B., Comaneci R.I., Cimpoesu N., Bujoreanu L.-G., *OAM-RC*, **4**, 6, 816 – 820 (2010).

ASPECTE MICROSTRUCTURALE NOI ALE PLĂCILOR DE MARTENSITĂ ÎN
ALIAJELE CU MEMORIA FORMEI PE BAZĂ DE Fe-Mn-Si ȘI Cu-Zn-Al

(Rezumat)

Au fost analizate din punct de vedere microstructural, prin intermediul microscopului cu scanare de electroni SEM, aspecte noi ale plăcilor de martensită din cadrul a două aliaje cu memoria formei pe bază de Fe-Mn-Si-Cr-Ni și respectiv Cu-Zn-Al. Evaluările structurale au evidențiat dimensiunile mai mari ale plăcilor de martensită ϵ hcp din cadrul aliajului cu memoria formei pe bază de Fe-Mn-Si-Cr-Ni, decât cele ale plăcilor de martensită ortorombică β_2 (9R), din cadrul aliajului cu memoria formei pe bază de Cu-Zn-Al. Analizele 3-D au fost efectuate în scopul evidențierii aspectelor înălțimilor și lățimilor plăcilor, ale ambelor tipuri de martensită ϵ hcp și β_2 9R. Au fost efectuate micrografii SEM dar și micrografii generale 3-D pentru a observa aspectele microstructurale ale ambelor sisteme de aliaje.

BULETINUL INSTITUTULUI POLITEHNIC DIN IAȘI
Publicat de
Universitatea Tehnică „Gheorghe Asachi” din Iași
Tomul LVIII (LXII), Fasc. 2, 2012
Secția
ȘTIINȚA ȘI INGINERIA MATERIALELOR

Fe BASIS BIOMATERIALS FOR DEGRADABLE CORONARY STENTS

BY

MIHAELA RĂȚOI*, SERGIU STANCIU and ROMEU CHELARIU

“Gheorghe Asachi” Technical University of Iași
Faculty of Material Science and Engineering

Received: February 29, 2012

Accepted for publication: March 19, 2012

Abstract: The studies carried out so far showed that the biodegradable metallic materials based on Fe have a potential application in the coronary stents field, but some caution should still be kept. Questioning the reliability of the biodegradable materials placed in the organism, it is required a particular attention: all implants have to fulfill the specification of the biocompatibility, biofunctionality, biodurability and biosecurity for a short, medium and long term (Erne *et al*, 2006).

The synthesis of some biodegradable metallic materials for temporary medical applications and the control of their biodegradation are areas of research that have been recently explored in the materials science field. At present, only a couple of biodegradable metallic materials based on iron have been investigated. Although the results are encouraging, it is necessary to continue this research and, more importantly, for this research is to have as a starting point a new approach concerning the biodegradability control.

Keywords: biodegradable stents; biocompatibility; Fe–Mn–Si alloys; PLD technique.

* Corresponding author: *e-mail*: mihaela.ratoi@yahoo.com

1. Introduction

Peuster *et al.* (2001) implanted for the first time in vivo, using a model with animals, a degradable stent based on pure commercial Fe. Even if afterwards the increase of work number concerning the degradable stents based on iron was relatively low, however, in the last 5 years there was an increase on this topic from various perspectives (Bujoreanu *et al.*, 2008; Bailey, 2009; Nie *et al.*, 2010; Hermawan *et al.*, 2010; Hermawan *et al.*, 2007; Liu *et al.*, 2011; Zhu *et al.*, 2009; Moravej *et al.*, 2010; Mueller *et al.*, 2006; Waksman, 2008; Erne *et al.*, 2006; Bujoreanu, 2002; Bujoreanu *et al.*, 2004; Van Humbeeck & Stalmans, 1998; Eggeler, 2004; Baruj *et al.*, 2004; Sawaguchi *et al.*, 2005; Dong *et al.*, 2005). The most investigated among the degradable materials based on Fe has been pure Fe (Baruj *et al.*, 2004; Sawaguchi *et al.*, 2005; Schinhammer *et al.*, 2010; Hermawan *et al.*, 2010, 2007; Erne *et al.*, 2006) or pure electroformed Fe (Bujoreanu *et al.*, 2004; Van Humbeeck & Stalmans, 1998; Eggeler, 2004), followed by alloys from the system Fe-Mn (Hermawan *et al.*, 2010; Liu *et al.*, 2011; Zhu *et al.*, 2009; Baruj, 2004), Fe-Mn-Pd (Liu *et al.*, 2011), Fe-Mn-Si (Moravej *et al.*, 2010), and Liu and Zheng (2006) investigated the influence of various alloying elements on Fe biodegradability and biocompatibility in vitro.

2. Arguments for Selecting this Project Topic

The studies carried out highlight the following aspects concerning the use of materials based on Fe for biodegradable stents:

1. Both pure Fe and its alloys have mechanic properties values close to those of the non-corrosive steel 316L, considered as the gold standard for permanent metallic stents; an exception is the alloying with Sn that has an undesirable effect on the mechanical behavior (Mueller *et al.*, 2006); values of the flow and tensile strength comparable to those of the non-corrosive steel 316L, but also a maximum extension is advisable for stents.

2. The alloying with elements that increase the austenite proportion is advisable from the perspective of using the magnetic resonance imagery (Nie *et al.*, 2010).

3. The corrosion degradation speed could be controlled by means of the synthesis method (Zhu *et al.*, 2009; Moravej *et al.*, 2010; Mueller *et al.*, 2006; Bujoreanu, 2002, 2004; Van Humbeeck & Stalmans, 1998; Eggeler, 2004), by alloying elements and the chemical compositions (Nie *et al.*, 2010; Liu *et al.*, 2011; Zhu *et al.*, 2009; Moravej *et al.*, 2010; Mueller *et al.*, 2006), the performed thermal and thermo-mechanic treatments (Hermawan *et al.*, 2007; Liu *et al.*, 2011; Zhu *et al.*, 2009; Moravej *et al.*, 2010; Mueller *et al.*, 2006; Bujoreanu, 2002, 2004; Van Humbeeck & Stalmans, 1998; Eggeler, 2004); the

corrosion speed is highly dependent on the material texture (Bujoreanu, 2002, 2004; Van Humbeeck & Stalmans, 1998; Eggeler, 2004). Even though progress has been made in the control of the degradation speed in vitro, however it wasn't found any clear solution concerning the control of degradability in vitro and in vivo of metallic materials based on Fe stents (Hermawan *et al.*, 2007; Liu *et al.*, 2011; Zhu *et al.*, 2009; Moravej *et al.*, 2010; Mueller *et al.*, 2006; Waksman, 2008; Erne *et al.*, 2006; Bujoreanu, 2002, 2004; Van Humbeeck & Stalmans, 1998; Eggeler, 2004).

4. The biocompatibility of the studied degradable metallic materials based on iron has to be evaluated in close connection with the degradation speed and the structure integrity maintenance up to the end of the vascular healing and remodeling process; the biodegradation implies Fe oxidation to ferrous or ferric ions, and the ions dilution in the biologic environment. The thrombogenicity and the neointimal proliferation have been reduced and no sign of local toxicity has been noticed. The endothelialisation of Fe stent has also been noticed in the models on animals (Bujoreanu *et al.*, 2008).

From a theoretical perspective, an ideal biodegradable stent should have inert behavior and be fully functional up to the end of the physiological processes of normal healing and vascular remodeling; then it must be removed as soon as possible through natural mechanisms specific to the human body. In the implantation first part, due to the necessity of a high degradation speed, the possibility of occurrence of local and systemic effects increases and, hence, one must pay special attention to the degradation products and to the speed at which they are formed and metabolized.

The degradation of the metallic stents is an actually in vivo corrosion process. Given the connection between degradation and functioning, it thus results that the securing of normal functioning until the completion of vascular remodeling (6...12 months after the implant) depends on the absence of corrosion or on the existence of uniform corrosion at small speed of the metallic material that the implanted stent is made of. The use of a material with a higher corrosion speed from the very first stage would lead to the increase of the thickness of the structural elements. This solution is unacceptable as we all know that such structural elements lead to side effects that cause the stent implant to fail.

Local and systemic biocompatibility must be guaranteed during the functioning period, as well as during the degradation one.

3. Objectives

The general objective of the project is to identify at least a galvanic couple comprised of metallic materials based on iron which, if used as multilayer material for temporary coronary stents, would facilitate the control of biodegradability in the above mentioned direction. Up to now, this approach

with regard to the control of the biodegradation of metallic materials based on Fe does not appear in the studied literature.

A fundamental requirement for temporary metallic stents is to have, throughout the entire implant duration, a biocompatible behavior, without side effects on the health condition of the patient subjected to such a treatment.

The achievement of the proposed objectives will generate new scientific knowledge concerning the behavior of Fe based metallic materials in simulated physiological environments specific to the medical application, an area of research that is relatively new, with a limited number of scientific papers in major publications. The characterization of the mechanic behavior of these materials is of vital importance for obtaining a stent with major clinical performances.

Novelty of materials besides technical solutions to control the speed of degradation is the property of shape memory effect that provides elements functionality.

There are two ways to control the rate of biodegradation, first by alloying addition elements (Mn, Si, Ca, Mg) of materials with shape memory effect and second by layers deposited structure, Fig. 1.

In Fig. 1 *a* material (different layers) is deposited as flat and the device will be made by welding and assembly and in Fig. 1 *b* layers are deposited on a support tube (removable type) device.

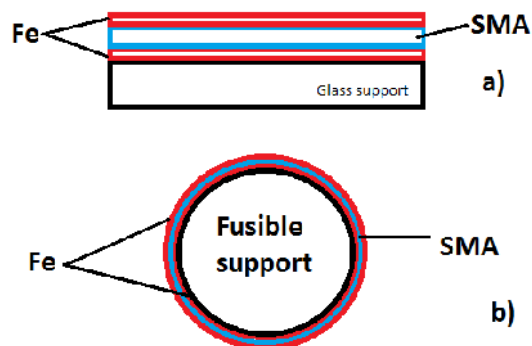


Fig. 1 – Schematic diagram of the structure layers of biodegradable shape memory material; *a* – plan and *b* – tube shape.

The most promising candidates to shape memory steels are Fe–Mn–Si alloys. The development of shape memory alloys belonging to the Fe–Mn–Si system started in 1982 with the attention of a perfect SME in single crystals

(<http://www.ruhr-uni-bochum.de/ww>). Owing to the fact that Mn stabilizes γ phase and Si decreases stacking fault energy while increasing austenite yield stress, an almost perfect SME could also be obtained in polycrystals, in the range Fe-(28-34) Mn-(4-6,5) Si (wt. %) (Baruj *et al.*, 2004). The main factor that stopped the development of these alloys, during almost 2 decades, was the necessity to apply a special thermomechanical treatment of training, in order to obtain a perfect SME. In the case of Fe-Mn-Si SMAs, training consists in applying several thermomechanical cycles comprising room temperature (RT)-deformation (producing each time an additional amount of stress induced martensite) and heating above the finish temperature of reverse martensitic transformation (Af) (Baruj *et al.*, 2004).

The materials based on iron-manganese are able to develop larger recovery stresses, have higher workability and weld ability and are cheaper than Ti-Ni SMAs. Fe-Mn based alloys, with concentrations of 10...30% Mn, have a reversible martensitic transformation γ (fcc) – ε (hcp). The existence of SME is connected to the obtainment of ε stress induced martensite, favored by the increase of the Mn amount in the expense of α' ferromagnetic martensite (Kim *et al.*, 2004). Presently, intensive efforts are carried out at the National Institute of Materials Science, in Ibaraki, Japan for the development of Fe-Mn-Si SMAs nano-particulated with NbC that enable damping behavior and make the alloys able to be used for seismic protection (Kim *et al.*, 2004). The main short coming of Fe-Mn-Si SMAs is that a SME of nearly 100% cannot be obtained unless several cycles of deformation by stress induced transformation (fcc-hcp) on mechanical loading and reversion (hcp-fcc) by heating is applied (Bujoreanu *et al.*, 2007).

In literature no iron based shape memory alloys through pulsed laser deposition (PLD) are recorded even though PLD represent a versatile technique.

Pulsed Laser Deposition (PLD) technique seems to be the natural choice since it demonstrated to be a versatile technique for thin films and multilayer processing with a high diversity of structural and morphological characteristics (Pulsed Laser Deposition of Thin Films, 1994, 2007). Many independent parameters can be changed under control in order to select the optimum deposition regimes of some specific structures and thin films. Growing thin films by PLD has numerous advantages:

a) the target composition can be reproduced. It is possible due to the congruent vaporization to deposit materials with complex chemical composition (Hermann *et al.*, 2010);

b) the sequential nature of the PLD process allows for a very precise control of the films thickness (10^{-1} A/pulse);

c) any type of material can be ablated, so the method is not limited to special classes of compounds;

d) using a carousel system with targets of different compositions, multilayer films can be obtained. The combinations are endless and new

composite materials with new, improved properties can be obtained (Ortega *et al.*, 2006);

e) the target is irradiated by light, so no contamination/ impurification occurs during the deposition process;

f) by varying the deposition parameters, drastically different structures can be obtained in terms of macroscopic and microscopic aspect, crystalline status and physical properties;

g) the number of pulses dictates if the ablated substance is deposited on substrate as thin films or as isolated nanoparticles and thus complex structures films/particles can be synthesized (Socol *et al.*, 2007).

There are however some disadvantages of PLD which are reminded in literature (Greer, 2006; Sima *et al.*, 2001; Yoshitake & Nagayama, 2004; Yoshitake *et al.*, 2002; György *et al.*).

Applications of the technique are many and various: complex oxide thin films for superconductors ($\text{YBa}_2\text{Cu}_3\text{O}_7$ (Develos-Bagarinao *et al.*, 2004), $\text{Ba}_2\text{Co}_2\text{Fe}_{12}\text{O}_{22}$ (Sudakar *et al.*, 2003)), chalcogenide thin layers (Petkova *et al.*, 2009), active mediums (Er:YAG (Liu & Zheng, 2011)), metal oxides for optical gas sensors (Eggeler, 2004; Schinhammer *et al.*, 2010; Liu & Zheng, 2011; Mani *et al.*, 2007; O'Brien *et al.*, 2009; Purnama *et al.*, 2010), protective coatings and barriers (*e.g.* AlN (Bakalova *et al.*, 2006; Nelea *et al.*, 2002), TiN, ZrC (Nelea *et al.*, 2002)), biocompatible coatings (prostheses coatings, particles for drug delivery), metallic oxides nanoparticles for fuel cells, and films or nanoparticles as antimicrobial and antibacterial protective barrier for medical application.

By MAPLE were obtained remarkable results in case of proteins like Immunoglobulin or Creatinine, a protein produced by muscles and released into blood. There were also successfully transferred materials like Poly (D,L-Lactide) for Controlled-Release Drug Systems (Bakalova *et al.*, 2006), polysaccharide derivates like Cinnamate-Pullulan and Tosylate-Pullulan for pharmaceutical applications (Develos-Bagarinao *et al.*, 2004).

Typical MAPLE setups comprise the vacuum chamber and a pulsed high-power laser system in operation in Laser-Surface-Plasma Interaction Laboratory (NILPRP) (Sima *et al.*, 2011; Crăciun *et al.*, 2011; Grigorescu *et al.*). Thin films of biomolecules and/or biopolymers with drug delivery properties could be grown on top of the metal alloys to form hybrid multilayered structures. The only difference compared to PLD is that in case of MAPLE technique the laser radiation is focused onto a cryogenic composite target consisting in 1...10% organic material dissolved in a solvent, at an incidence angle of the laser beam of 45° . During MAPLE deposition the target is rotated in order to avoid drilling and is kept at very low temperatures using copper braids connected to a liquid nitrogen reservoir.

The technique uses high energy laser pulses (typically 2~5 J/cm²) to melt, evaporate, and ionize material (ablation process) from the surface of a

target. This ablation event produces a transient, highly luminous plasma plume that expands rapidly away from the target surface. The vaporized material, containing neutrals, ions, and electrons, is known as a laser-produced plasma plume, and expands rapidly away from the target surface (velocities typically $\sim 10^6$ cm/s in vacuum). PLD allows obtaining mono- and multi-structures of any material onto a solid substrate, including flexible ones. The active substance is transported in plasma state from target to collector where ions and atoms attain high kinetic energy to synthesize an adherent layer able to sustain strong tensions without peeling or cracking.

Another approach of this project is the Combinatorial-PLD (C-PLD) method (György *et al.*; Sudakar *et al.*). In C-PLD, the targets are located in two different positions and ablated simultaneously, the material being collected on the same substrate (Fig. 2).

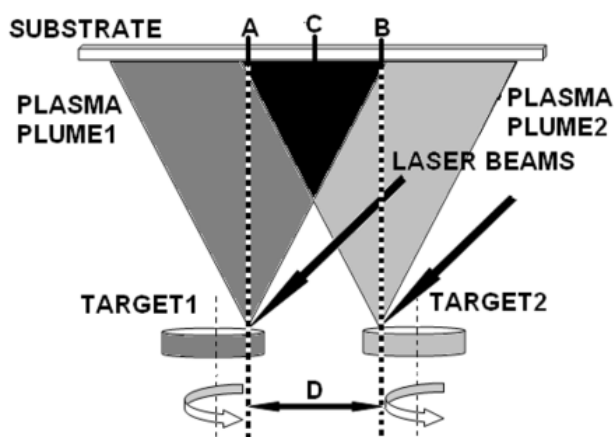


Fig. 2 – Combinatorial- PLD setup using two different targets.

Using C-PLD in this geometry we will be able to deposit films having well-defined composition gradients across the length of the substrate. The laser beam impinges the targets at a specific separation distance between the laser spots. A and B positions on the substrate correspond to mirror positions of the laser spots on the target 1 and target 2, respectively. Therefore, at A and B points we shall get the maximum of composition for the target 1 and 2: a gradient of composition from 100% M1 material to 100% M2 material. Point C represents the place where the two materials will be collected in equal proportions. One can generate this way a compositional library of the two materials in order to identify the optimum dosage for a certain application. We will focus on the Fe, Mn, Si alloys in order to find the best composition and accordingly, the shape memory properties. Moreover, Ca and Mg will be added knowing that these elements control the biodegradation process of these alloys.

Thin metallic materials (with reduced dimensions and mass) can be more easily investigated by biodegradation point of view based on combinatory investigation techniques (SEM/TEM (2D and 3D)+EDAX+(linear and cyclic) Potentiometry). As a research direction it is basically to analyze and observe the metallic material biodegradation influence on the shape memory materials properties in time to characterize the memory effect workability of the applicative elements until full degradation.

4. Conclusions

Obtaining a thin material with shape memory effect and biodegradability at the same time, many applicative problems can be solved using both properties at the same time. One of the solved problems will be considered to be the shape memory alloy material quantity and the encouraging low costs that will allow that industrial field to use and exploit this kind of new intelligent materials.

As the solution proposed by the project for the control of the biodegradation of temporary metallic coronary stents does not appear in the results presented in the studied literature, we expect a major scientific impact in this particular research field.

REFERENCES

- Bailey S.R., *DES Design: Theoretical Advantages and Disadvantages of Stent Strut Materials, Design, Thickness and Surface Characteristics*. J. Interv. Card., **22**, 1, 3-17 (2009).
- Bakalova S., Simeonov S., Kafedjijiska E., Szekeres A., Grigorescu S., Socol G., Axente E., Mihailescu I.N., *Plasma. Processes & Polymers*, **3**, 2, 205-208 (2006).
- Baruj A., Kikuchi T., Kajiwara S., Shinya N., *Improvement of Shape Memory Properties of NbC Containing Fe-Mn-Si-Based Shape Memory Alloys by Simple Thermomechanical Treatments*. Mater. Sci. an. Engng., **A 378**, 2004, 333-336.
- Baruj A., Kikuchi T., Kajiwara S., *TEM Observation of the Internal Structures in NbC Containing Fe-Mn-Si-Based Shape Memory Alloys Subejted to Pre-Deformation Above Room Temperature*. Mater. Sci. a. Engng., **A 378**, 2004, 337-342.
- Bujoreanu L.G., Dia V., Stanciu S., Susan M., Baciuc C., *Study of Tensile Constrained Recovery Behavior of a Fe-Mn-Si Shape Memory Alloy*. Europ. Phys. J., Special Topics, **158**, 15-20 (2008).
- Bujoreanu L.G., *Intelligent Materials* (in Romanian). Edit. Junimea, Iaşi, 2002.
- Bujoreanu L.G., Stanciu S., Dia V., Bull. Inst. Politehnic, Iaşi, **LIII (LVII)**, 1, s. Ştiinţa şi Ingineria Materialelor, 21 (2007).

- Bujoreanu L.G., Stanciu S., Munteanu C., Susan M., *Mechanical and Thermal Memory of Cu-Zn-Al Base Alloys*. Edit. POLITECHNIUM, Iași, 2004.
- Crăciun D., Bourne G., Zhang J., Siebein K., Socol G., Dorcioman G., Crăciun V., *Surface & Coatings Technol.*, **205**, 2011, 5493-5496.
- Develos-Bagarinao K., Yamasaki H., Nakagawa Y., Endo K., *Physica, C*, **412-414**, 2004, 1286-1290.
- Dong Z.Z., Kajiwara S., Kikuchi T., Sawaguchi T., *Acta mater.*, **53**, 4009 (2005).
- Eggeler G., *SFB 459-A Research Center for Progress in Understanding and New Applications of Shape Memory Alloys (SMAs)*. *Materialwissenschaft und Werkstofftechnik*, **35**, 5, 2004, 253-254.
- Erne P., Schier M., Resink T.J., *The Road to Bioabsorbable Stents: Reaching Clinical Reality?*. *Cardiovasc. Intervent. Radiol.*, **29**, 11-16 (2006).
- Erne P., Schier M., Resink T.J., *The Road to Bioabsorbable Stents: Reaching Clinical Reality?* *Cardiovasc Intervent Radiol.*, **29**, 11-16 (2006).
- Erne P., Schier M., Resink T.J., *The Road to Bioabsorbable Stents: Reaching Clinical Reality?* *Cardiovasc. Intervent. Radiol.*, **29**, 2006, 11-16.
- Greer J., *Large-Area Commercial Pulsed Laser Deposition*. In R. Eason (Ed), *Pulsed Laser Deposition of thin Films: Applications-Lead Growth of Functional Materials*. Wiley & Sons, New York, USA, 2006.
- Grigorescu S., Carradò A., Ulhaq C., Faerber J., Ristoscu C., Dorcioman G., Axente E., Werckmann J., Mihăilescu I.N., *Study of the gradual interface between hydroxyapatite thin films PLD grown onto Ti-controlled sublayers*, *Appl. Surface Sci.*, **254**, 4, (2007) 1150-1154.
- György E., Mihăilescu I.N., Kompitsas M., Giannoudakos A., *Thin Solid Films*, **446**, **2**.
- Hermann J., Mercadier L., Mothe E., Socol G., Alloncle P., *Spectrochim. Acta, Part B*, **65**, 636 (2010).
- Hermawan H., Dubé D., Mantovani D., *Development of Degradable Fe-35Mn Alloy for Biomedical Application*. *Advanced Materials Research*, **15-17**, 2007, 107-112.
- Hermawan H., Dubé D., Mantovani D., *Development of Degradable Fe-35Mn Alloy for Biomedical Application*. *Adv. Mater. Res.*, **15-17**, 2007, 107-112.
- Hermawan H., Purnama A., Dube D., Couet J., Mantovani D., *Fe-Mn Alloys for Metallic Biodegradable Stents: Degradation and Cell Viability Studies*. *Acta Biomaterialia*, **6**, 2010, 1852-1860.
- Hermawan H., Purnama A., Dube D., Couet J., Mantovani D., *Fe-Mn Alloys for Metallic Biodegradable Stents: Degradation and Cell Viability Studies*. *Acta Biomaterialia*, **6**, 2010, 1852-1860.
- Kim J.-C., Han D.-W., Baik S.H., Lee Y.-K., *Mater. Sci. Eng.*, **A 378**, 323 (2004).
- Liu B., Zheng Y.F., *Effects of Alloying Elements (Mn, Co, Al, W, Sn, B, C and S) on Biodegradability and in Vitro Biocompatibility of Pure Iron*. *Acta Biomaterialia*, **7**, 3, 1407-1420 (2011).
- Liu B., Zheng Y.F., Ruan L., *In Vitro Investigation of Fe₃₀Mn₆Si Shape Memory Alloy as Potential Biodegradable Metallic Material*. *Materials Letters*, **65**, 2011, 540-543.
- Mani G., Feldman M.D., Patel D., Mauli Agrawal C., *Coronary Stents: a Materials Perspective*. *Biomaterials*, **28**, 1689-1710 (2007).

- Moravej M., Prima F., Fiset M., Mantovani D., *Electroformed Iron as New Biomaterial for Degradable Stents: Development Process and Structure–Properties Relationship*. Acta Biomaterialia, **6**, 2010, 1726-1735.
- Mueller P.P. *et al.*, *Control of Smooth Muscle Cell Proliferation by Ferrous Iron*. Biomaterials, **27**, 2006, 2193-2200.
- Nelea V., Pelletier H., Iliescu M., Verckmann J., Crăciun V., Mihăilescu I.N., Ristoscu C., Ghica, J. Mater. Sci: Mater. Med., **13**, 2002, 1167-1173.
- Nie F.L., Zheng Y.F., Wei S.C., Hu C., Yang G., *In Vitro Corrosion, Cytotoxicity and Hemocompatibility of Bulk Nanocrystalline Pure Iron*. Biomed. Mater., **5**, 2010, 1-10.
- O'Brien B., Carroll W., *The Evolution of Cardiovascular Stent Materials and Surfaces in Response to Clinical Drivers: a Review*. Acta Biomaterialia, **5**, 945-958 (2009).
- Ortega N., Bhattacharya P., Katiyar R.S., *Solid. Mater. Sci. Engng.*, **B**, 1-3, 36-40 (2006).
- Petkova T., Popov C., Hineva T., Petkov P., Socol G., Axente E., Mihailescu C.N., Mihailescu I.N., Reithmaier J.P., *Appl. Surf. Sci.*, **255**, 5318-5321 (2009).
- Peuster M. *et al.*, *A Novel Approach to Temporary Stenting: Degradable Cardiovascular Stents Produced From Corrodible Metal*. Results 6–18 months after implantation into New Zealand white rabbits, **86**, 2001, 563–569.
- Purnama A., Hermawan H., Couet J., Mantovani D., *Assessing the Biocompatibility of Degradable Metallic Materials: State-of-the-Art and Focus on the Potential of Genetic Regulation*. Acta Biomaterialia, **6**, 1800-1807 (2010).
- Sawaguchi T., Kikuchi T., Yin F., Ogawa K., Kajiwara S., Kushibe A., Higashino M., Ogawa T., *Pseudoelasticity and Damping Properties Associated with fcc/hcp Martensitic Transformation in NbC Containing Fe-Mn-Si-Based Alloys*. Bul. Inst. Politehnic, Iaşi, **LI (LV)**, **4**, s. Ştiinţa şi Ingineria Materialelor, 1-11 (2005).
- Schinhammer M., Hänzi A.C., Löffler J.F., Uggowitzer P.J., *Design Strategy for Biodegradable Fe-Based Alloys for Medical Applications*. Acta Biomaterialia, **6**, 2010, 1705–1713.
- Sima F., Axente E., Ristoscu C., Kononenko T.V., Nagovitsin I.A., Chudinova G., Konov V.I., Socol M., Enculescu I., Sima L.E., Petrescu S.M., Mihăilescu I.N., *J. of Biomedical Mater. Res., Part A*, **96A**, 384-394 (2011).
- Sima F., Socol G., Axente E., Mihăilescu I.N., Zdrentu L., Petrescu S.M., Mayer I., *Biocompatible and bioactive coatings of Mn²⁺-doped β-tricalcium phosphate synthesized by pulsed laser deposition*, *Appl. Surface Sci.*, **254**, **4**, (2007), 1155-1159.
- Socol G., Axente E., Ristoscu C., Sima F., Popescu A., Stefan N., Escoubas L., Ferreira J., Bakalova S., Szekeres A., Mihailescu I.N., *J. Appl. Phys.*, **102**, 083103, 2007.
- Sudakar C., Subbanna G.N., Kutty T.R.N., *J. Appl. Phys.*, **94**, 2003, 6030-6033.
- Van Humbeeck J., Stalmans R., *Characteristics of Shape Memory Alloys*. In *Shape Memory Materials*, Otsuka K. and Wayman C.M. (Eds.), Cambridge Univ. Press, 1998, 149-183
- Waksman R., *Short-Term Effects of Biocorrosible Iron Stents in Porcine Coronary Arteries*. *J. of Interventional Cardiology*, **21**, **1**, 2008, 15-20.
- Wan J.F., Chen S.P., Hsu T.Y., Huang Y.N., *Mater. Sci. Eng.*, **A 438-440**, 887 (2006).

- Yoshitake T., Nagayama K., *Vacuum*, **74**, 3-4, 2004, 515-520.
- Yoshitake T., Shiraishi G., Nagayama K., *Appl. Surf. Sci.*, *197-198*, 2002, 379-383.
- Zhu S. *et al.*, *Biocompatibility of Fe-O Films Synthesized by Plasma Immersion Ion Implantation And Deposition*. *Surface & Coatings Technol.*, **203**, 2009, 1523-1529.
- Zhu S. *et al.*, *Biocompatibility of Pure Iron: In Vitro Assessment of Degradation Kinetics and Cytotoxicity on Endothelial Cells*. *Mater. Sci. a. Engng.*, **C 29**, 2009, 1589-1592.
- * * <http://www.ruhr-uni-bochum.de/ww>.
- * * *Pulsed Laser Deposition of Thin Films*. Edited by D.B. Chrisey and G.K. Hubler, Wiley & Sons, New York, USA, 1994.
- * * *Pulsed Laser Deposition of thin Films: Applications-Lead Growth of Functional Materials*. Edited by R. Eason, Wiley & Sons, New York, USA, 2007.

BIOMATERIALE PE BAZĂ DE Fe PENTRU STENTURI CORONARIENE DEGRADABILE

(Rezumat)

Studiile făcute până acum au arătat că materialele metalice biodegradabile pe bază de Fe au un potențial în aplicativitatea în domeniul stenturilor, însă trebuie luate în considerare niște precauții. Luând în discuție fiabilitatea materialelor biodegradabile implantate în organism, este necesară o atenție particulară: toate implanturile trebuie să îndeplinească condiția de biocompatibilitate, biofuncționalitate, biodurabilitate și biosecuritate pentru o perioadă scurtă, medie sau lungă de timp.

Sinteza unor materiale metalice biodegradabile, pentru aplicații medicale temporare cât și controlul biodegradării lor sunt domenii de cercetare care au fost exploatate recent în domeniul științei materialelor. În prezent, au fost investigate doar o parte din materialele metalice biodegradabile din Fe. Deși rezultatele sunt încurajatoare, este necesar să se continue această cercetare, mai important fiind faptul că este nevoie de o nouă abordare de la început în ceea ce privește controlul biodegradabilității.

BULETINUL INSTITUTULUI POLITEHNIC DIN IAȘI
Publicat de
Universitatea Tehnică „Gheorghe Asachi” din Iași
Tomul LVIII (LXII), Fasc. 2, 2012
Secția
ȘTIINȚA ȘI INGINERIA MATERIALELOR

CONSIDERATIONS REGARDING STRUCTURAL CHARACTERISTICS AND PROPERTIES OF TITANIUM BASED DENTAL ALLOYS

BY

ELENA-RALUCA BACIU*, IRINA GRĂDINARU, MARIA BACIU¹ and
NORINA CONSUELA FORNA²

“Gr. T. Popa” University of Medicine and Pharmacy of Iași,
Department of Dental Materials

²Department of EPI Clinic and Therapy

“Gheorghe Asachi” Technical University of Iași

¹Department of Material Engineering and Industrial Security

Received: February 29, 2012

Accepted for publication: March 19, 2012

Abstract: Microstructural researches on Ti-based alloys under analysis aimed at identifying the main structural constituents that will influence their subsequent behaviour during the finishing processes by mechanical polishing. The aluminum and niobium alloy determined the modification of structural constitution in case of Biotan™ Nb alloy, since the two solid solutions formed are characterized by high values of microhardness, a fact that will lead to a more difficult mechanical finishing.

Keywords: Ti-based alloys; microstructure; microhardness.

1. Introduction

Metallographic structure plays an important role in terms of resistance to corrosion and technological properties of dental alloys.

* Corresponding author: *e-mail*: raluca_baciu@yahoo.com

The catalogues of the manufacturing companies and the technical charts of the product exhibit only general information related to some properties of dental alloys insisting more on the processing manner and the fields of use.

2. Goal of Researches

To appreciate the behaviour of the dental alloys studied in the processes of mechanical polishing, it is necessary to carry out their microstructural analysis and determine the microhardness of the superficial layer. It is obvious that alloys having higher microhardness will be more difficult to process by chipping, a technology through which mechanical finishing is performed (grinding and polishing) of metal components of prosthetic devices.

Microstructural researches on dental alloys under study aimed at identifying the main structural constituents that will influence the subsequent behaviour of the materials during the finishing processes by mechanical polishing of the exterior surfaces of metal components of prosthetic devices.

3. Material and Method

Microstructural investigations were carried out on the frontal surface of cylindrical test tubes ($\varnothing 7 \times 10$ mm) made of Biotan™ Nb and Biotan™ Titanium.

The metal specimens were inserted by hot pressing into epoxidic resin (Fig.1).

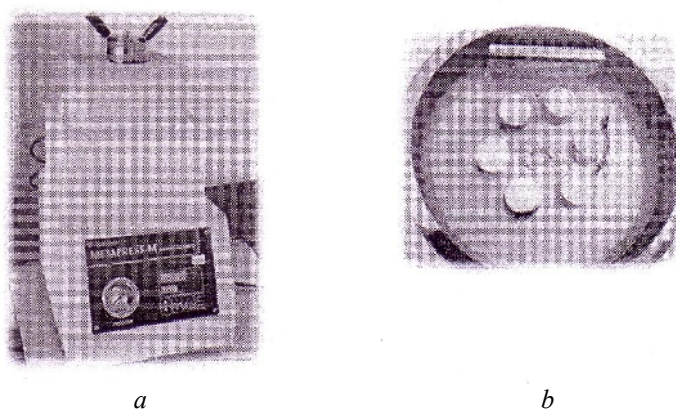


Fig. 1 – Preparing specimens for microstructural analyses;
a – Metapress-M (Metkon, Turkey) mechanical press; *b* – metallographic specimens after insertion into epoxidic resin.

After insertion into epoxidic resin, the frontal surface of specimens was mechanically processed by mechanical grinding on metallographic paper with

different granularities of abrasive particles. The operation of mechanical polishing was carried out on felt soaked with an emulsion based on abrasive particles having sizes specific to ultra-polishing or micro-polishing (Table 1, Fig. 2).

Table 1
Grinding and Polishing Conditions for Metallographic Specimens

Alloy class	Grinding by abrasive paper	Felt ultra-polishing	Felt micro-polishing	Pan rotation speed, [rpm]	Processing time, [min]
Titanium-based alloys Biotan [®] and Biotan Nb	<ul style="list-style-type: none"> • 320-P(400); • SiC; • water cooling; 	<ul style="list-style-type: none"> • diamond particle suspension; • particle size 9 μm; 	<ul style="list-style-type: none"> • SiC particle suspension; • particle size 0.05 μm; 	<ul style="list-style-type: none"> • 240...300 – for grinding; • 120...150 – for ultra-polishing and micro-polishing; 	<ul style="list-style-type: none"> • 10 – for ultra-polishing; • 10 – for micro-polishing;



a



b

Fig. 2 – Equipment for the mechanical processing of frontal surfaces of metallographic specimens; *a* – Forcipol 1V machine (Metkon, Turkey – for grinding; *b* – Metkon[®] 1V machine (Metkon, Turkey) – for polishing.

To carry out the microstructural tests, the polished surface of each metallographic specimen was attacked by a chemical reagent. The chemical reagents used were chosen in accordance with the chemical composition of alloy (Table 2) so as to highlight every microstructural detail: grain limits, type of structural constituents, nature of structural transformations occurred etc.

Table 2*Reagents Used for the Chemical Attack of Specimens from Dental Non-Noble Alloys*

Alloy class	Chemical reagent	Observations
Titanium-based alloys (Biotan™ Titanium and Biotan™ Nb)	100 ml water; 1...3 ml HF; 2...6 ml HNO ₃ .	Kroll reagent; attack by tamponing: 3...10 s; immersion attack: 10...30 s.

Microstructural researches were conducted on metallographic microscope Neophot® 21 (Germany) (Fig. 3).



Fig. 3 – Optical metallographic microscope Neophot® 21 – bird's-eye view.

Determinations related to microhardness were conducted on the same surface of specimens on which we conducted the microstructural tests.

Measuring Vickers microhardness represents a very precise method of determination of hardness of different structural constituents, simultaneously with metallographic analysis.

Experimental assays were conducted on Neophot® 21 microscope provided with a special device for microhardness determination (Hanemann device).

All microhardness determinations were carried out in similar conditions by using a pressing force $F = 1$ N specific to hardness $HV_{0.1}$.

4. Results and Discussions

Microstructural investigations were conducted in light field at different magnification powers of the lens-eyeglass-camera optical system.

Biotan™ Titanium material has a microstructure specific to pure metal (titanium – 1st class), with elongated crystalline grains – of light colour and grey inter-crystalline limits (Fig. 4).

Being a titan-based biphasic alloy (Ti-6Al-7Nb), Biotan™ Nb material has a structure made of solid solutions α and β . The crystalline grains have an

acicular aspect and they are white (solid solution α – based on $Ti_{\alpha}Nb$) and grey (solid solution β – $Ti_{\beta}Nb$) (Fig. 5).



Fig. 4 – Microstructure of Biotan™ Titanium material – magnification power 1,000:1.

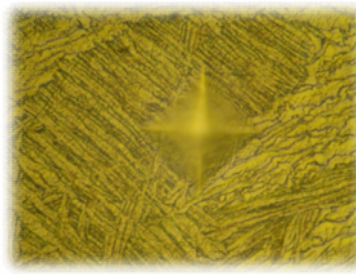


Fig. 5 – Microstructure of Biotan™ Nb alloy (Ti-6Al-7Nb) – magnification power 1000:1

Experimental investigations for the determination of microhardness of dental non-noble alloys under study were carried out simultaneously with the microstructural analysis of each metallographic specimen.

Biotan™ Titanium represents pure titanium metal – 1st class being characterised by a high purity level. Microhardness determinations conducted are presented in Table 3, and the penetrator's impressions are shown in Fig. 4.

Table 3
Microhardness Values for Biotan™ Titanium Material

Impression no.	Divisions of microscope eyeglass	Impression diagonal, [μ m]	Tested area	Microhardness, $HV_{0.1}$
1	140	24.92	grey grain limit	299
2	138	24.56	white crystalline grain	307
3	137	24.39	white crystalline grain	312
4	141	25.10	grey grain limit	294
5	146	25.99	grey grain limit	275
6	136	24.21	white crystalline grain	316

The average values of microhardness confirm the fact that the grain limits (the grey areas) are characterized by lower mechanical and chemical resistance as compared to crystalline grains: $HV_{0.1} \cong 310$ for crystalline grains and $HV_{0.1} \cong 289$ for grain limit.

As for Biotan™ Nb alloy, microhardness measurements highlighted the hardening effect of titanium alloying with aluminum and niobium on the solid solutions based on Ti_{α} or Ti_{β} , Table 4, and Fig. 5, respectively.

Table 4
Microhardness Values for Biotan™ Nb Alloy

Impression no.	Divisions of microscope eyeglass	Impression diagonal, [μm]	Tested area	Microhardness, $HV_{0.1}$
1	125	22.25	white grains (areas)	375
2	126	22.43	white grains (areas)	369
3	135	24.03	grey grains (areas)	321
4	128	22.78	grey grains (areas)	357
5	127	22.61	white grains (areas)	363
6	123	21.89	white grains (areas)	387

We may notice that the two solid solutions $Ti_{\alpha}(Nb)$ and $Ti_{\beta}(Nb)$ have quite equal microhardness average values: $HV_{0.1}$ – for $Ti_{\alpha}(Nb) \cong 374$ and $HV_{0.1}$ – for $Ti_{\beta}(Nb) \cong 339$. The presence of the precipitation phenomenon in solid solution $Ti_{\alpha}(Nb)$ and the formation of Ti_3Al particles explain the slightly higher values of microhardness for this structural constituent.

5. Conclusions

The microstructural researches conducted on dental non-noble alloys allowed us to formulate the following conclusions:

1. Having the chemical structure specific to pure metal Titanium–1st class (ASTM B265), Biotan™ Titanium material has its microstructure made of titanium crystalline grains of elongated shape and sinuous limits.

2. As for Biotan™ Nb, it has a microstructure made of crystalline grains of acicular shape for the two solid solutions based on titanium $Ti_{\alpha}(Nb)$ and $Ti_{\beta}(Nb)$ resulted from the alloying with aluminum and niobium.

3. Biotan™ Titanium material is characterized by almost uniform values of microhardness, as aspect corresponding to the structural constitution made only of crystalline grains of pure metal.

4. The alloying with aluminum and niobium determined the modification of the structural constitution of Biotan™ Nb alloy, the two solid solutions formed being characterized by higher values of microhardness, as compared to Biotan™ Titanium material.

5. The value differences between average microhardnesses of the two materials from the class of titanium-based allows are not very big ($HV_{0.1}$ Biotan™ Nb = 357 and ($HV_{0.1}$ Biotan™ Titanium = 301) because the reduced quantities of alloying elements (6% Al and 7% Nb) did not allow for the formation of specific intermetallic compounds Ti_3Al , Nb_2Al and Al_3Nb , which are hard and fragile.

6. Biotan™ Nb alloy will be more difficult to finish due to its structure made of the two solid solutions characterized by high values of microhardness.

REFERENCES

- Ardelle A.J., *Metallic Alloys Experimental and Theoretical Perspectives*. Kluwer Acad. Publ., Olanda, 1994, 93.
- Andronache M., Forna N., *The Study of the Distribution of Tensions and Deformations of Removable Partial Dentures*. Revista română de stomatologie, **LVI**, 4, 272-275 (2010).
- Barbosa P.F., Button S.T., *Microstructure and Mechanical Behaviour of the Isothermally Forged Ti-6Al-7Nb Alloy*. Proc. of the Inst. of Mechan. Engineers Part L. J. of Mater.: Design a. Appl., 2000, <http://pil.sagepub.com/content/214/1/23>.
- Craig R.G., *Materiale dentare restaurative* (tr. lb. română). Edit. All Education, București, 2001.
- Ghiban B., *Metallic Biomaterials*. Edit. Printech, București, 1999.
- Stelea O., Panaite Șt., Morariu C., *Metalurgie stomatologică și biomateriale*. Edit. Apollonia, Iași, 2000.
- Wang R.R., Fenton A., *Titanium for Prosthodontic Applications*. Rev. Quintessence Dental Technology, **27**, 401-408 (1996).
- Wataha J.C., Regina L.M., *Casting Alloys*. The Dental Clinics of North America, **48**, 499-512 (2004).
- Wataha J.C., *Alloys for Prosthodontic Restorations*. J. Prosthet Dent, **87**, 351-363, (2002).

CONSIDERAȚII PRIVIND CARACTERISTICILE STRUCTURALE ȘI
PROPRIETĂȚILE ALIAJELOR DENTARE CU BAZA TITAN

(Rezumat)

Cercetările microstructurale asupra aliajelor pe bază de Ti investigate au avut ca scop identificarea principalilor constituenți structurali care vor influența comportamentul ulterior al acestora la prelucrările de finisare prin lustruire mecanică. Alierea cu aluminiu și niobiu a determinat modificarea constituției structurale în cazul aliajului Biotan™ Nb, cele două soluții solide formate fiind caracterizate prin valori mai mari ale microdurității fapt care va determina o finisarea mecanică mai dificilă.

BULETINUL INSTITUTULUI POLITEHNIC DIN IAȘI
Publicat de
Universitatea Tehnică „Gheorghe Asachi” din Iași
Tomul LVIII (LXII), Fasc. 2, 2012
Secția
ȘTIINȚA ȘI INGINERIA MATERIALELOR

STEEL – BRONZE BIMETAL BY IMMERSION AND VERTICAL CENTRIFUGATION

BY

CONSTANTIN CORĂBIERU*, DAN DRAGOȘ VASILESCU¹,
ANIȘOARA CORĂBIERU¹ and PETRICĂ CORĂBIERU¹

“Gheorghe Asachi” Technical University of Iași
Department of Material Engineering and Industrial Security
¹SC PROCOMIMPEX, Iași

Received: February 29, 2012

Accepted for publication: March 19, 2012

Abstract: The joining temperature is the most important metallurgic factor that influences the characteristics and structure of the bimetallic layers obtained by immersion and vertical centrifugation. In order to outline the influence of the joining temperature, a series of parameters have been held constant, and assessments for different values of the joining temperature have been performed. Proper outcome was obtained at joining temperatures ranging between $T_{\text{join}} = 1,100^{\circ}\text{C}$ and $T_{\text{join}} = 1,160^{\circ}\text{C}$.

Keywords: steel – bronze bimetal; immersion – vertical centrifugation.

1. Introduction

The originality of this way of obtaining steel-bronze bimetal jacks by immersion and vertical centrifugation (ICV) consists in its complete national novelty. The ICV procedure contributes to elimination of certain operations and equipment require for the pre-heating, handling of liquid metal, casting in

* Corresponding author: *e-mail*: constantin.corabieru@yahoo.com

classical centrifugal machines, and extraction. The ICV process allows full automation, crossing and overlaying of the production processes – the deposition one and the bar and parts casting (Corăbieru & Corăbieru, 2004; Velicu *et al.*, 2008).

2. Experimental Procedure

The technological experimental principle for execution of steel-bronze bimetallic jacks consists of the immersion of the steel core in the bronze dip, lifting the core out of the dip until about half its length and its spinning with an appropriate angular speed required for the deposition to take place. The centrifugal force that appears by spinning the core in the bronze dip determines the repartition of the bronze on the core steel walls, the adherence of the bronze layer and the diffusion of the atoms at the steel-bronze interface, thus creating an inter-phase zone. The principle schema of executing bimetallic jacks by vertical centrifugation is presented in Fig. 1. The steel jack is immersed in the bronze dip and its spinning begins (Corăbieru *et al.*, 2007).

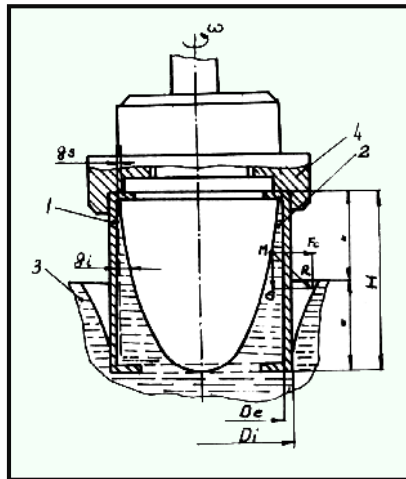


Fig. 1 – Principle scheme of the ICV process: 1 – steel core; 2 – the bronze layer distributed on the core walls; 3 – the bronze dip; 4 – fastening chuck.

In the beginning time of the deposition process, the melted bronze does not have the angular speed uniform in all its layers, but gradually this speed gets uniformed and becomes equal to the angular speed of the steel core. It is under these conditions that the spinning movement is stabilised and one can reckon that the spinning melted bronze finds itself in a relative rest situation, the space form of the free surface being a rotational paraboloid. After stabilising the spinning movement, the jack is gradually lifted up so that, when the optimal

deposition speed is reached, the jack is immersed only a hint in the bronze dip. (Corăbieru *et al.*, 2007).

3. The Vertical Centrifuge Machine MC

The designed and built MC is the main device of the installation for execution of bimetallic jacks. The MC ensures the transport of the steel core to each and every working point of the equipment, executes the immersion of the jack core in the IDP, the CTI, and in IR, as well as the spinning movement of the jack in the bronze dip in view of executing the deposition by ICV. In Fig. 2, the MC and its designed principle scheme are presented.

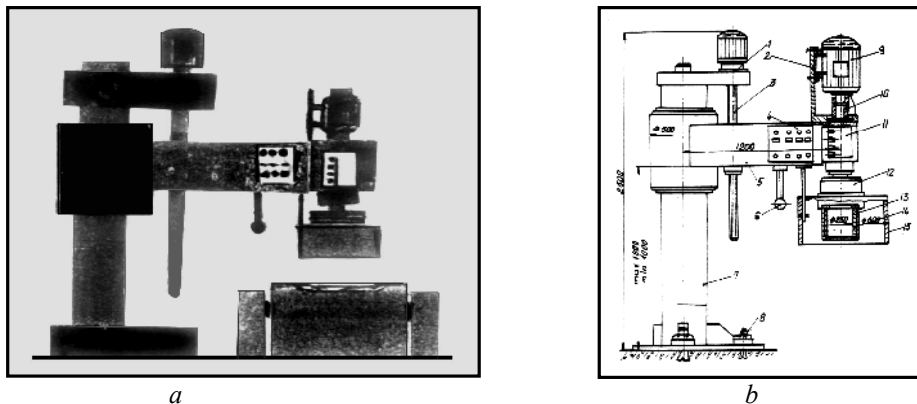


Fig. 2 – The centrifuge machine MC; *a* – the vertical centrifuge machine for execution of bimetals by ICV; *b* – the principle scheme of the designed and built MC: 1 – motor reduction gear for vertical movement; 2 – support for electric dc engine; 3 – screw-nut mechanism for vertical movement; 4 – Control panel; 5 – folding arm; 6 – handle; 7 – guiding axis; 8 – foundation bolts; 9 – Dc engine; 10 – coupling; 11 – main shaft; 12 – mechanic lathe; 13 – steel jack; 14 – deposited bronze layer; 15 – sliding cylindrical gasket.

4. Determination of the Specific Adherence

The specific adherence characterizes the bimetallic component parts for automobiles from a qualitative point of view. For the calculation of the specific adherence the resistance of detachment by shearing is necessary to be determined (Corăbieru *et al.*, 2007).

In the Fig. 4, types of specimens used for the proposed modalities of determination of the detachment resistance by shearing are shown.

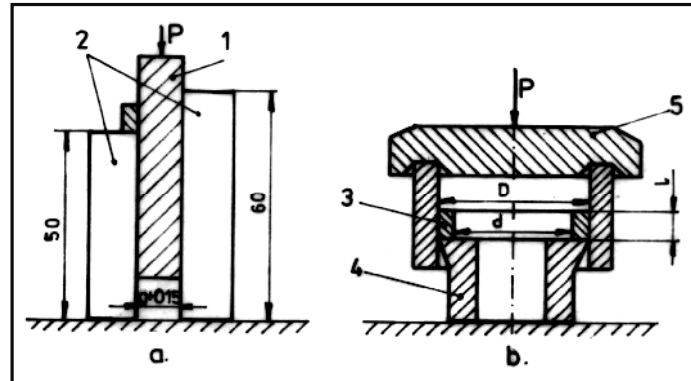


Fig. 3 – Proposed modalities of determination of the detachment resistance by shearing; *a* – determination of the detachment resistance with linear test bar: 1 – linear test bar; 2 – guiding stocks; *g* – structure of base support of OLT 35; *b* – determination of the detachment resistance with circular test bar: 3 – circular test bar type bushing-disc; 4 – matrix; 5 – superior support; *D* – inner diameter of base support of the bimetallic bushing; *d* – inner diameter of the bimetallic bushing.

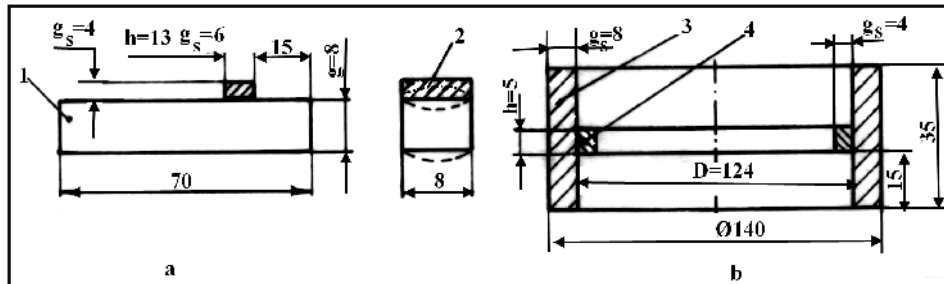


Fig. 4 – Types of specimens used for the proposed modalities of determination of the detachment resistance by shearing of the experimented bimetallic bushings; *a* – linear specimen: 1 – base material OLT35; 2 – bronze layer deposited by vertical spin casting, $g_s = 4$ mm; *A* – the aria of the surface submitted to the detachment by shearing, $A = h \times 8 = 1.5g_s \times 8 = 1.5 \times 4 \times 8 = 48 \text{ mm}^2$; *b* – circular specimen type bushing-disc; 3 – support of base steel OLT 35, $\Phi 140 \times 8$; 4 – bronze layer deposited by vertical spin casting, $g_s = 4$ mm; *D* – inner diameter of the base support, [mm]; *h* – height of the deposited layer submitted to the detachment, [mm]; *A* – aria of the surface submitted to the detachment by shearing, $A = \pi Dh = \pi \times 124 \times 5 = 1,946.8 \text{ mm}^2$.

The specific adherence, q , is determined with the formula

$$q = F/A, [\text{N}/\text{mm}^2],$$

where: F is the pressing or tensile force, [N]; A – aria of the surface submitted to the detachment, $[\text{mm}^2]$.

Depending on the specific adherence value q , we can have:

- a) soft joint: $q < 70 \text{ N/mm}^2$;
- b) average joint: $q = 70 \dots 170 \text{ N/mm}^2$;
- c) strong joint: $q > 170 \text{ N/mm}^2$.

5. Experimental Results

For the spotlight of the influence of the joining temperature into the framework of the experiments, the following parameters have been kept constant:

- a) dimensions of the base half-product $\Phi 140 \times 8 \text{ OLT } 35$;
- b) deposited bronze layer: superior thickness $g_s = 4 \text{ mm}$; inferior thickness $g_i = 12 \text{ mm}$; final thickness after machining $g_0 = 4 \text{ mm}$;
- c) length of steel support $L = 140 \text{ mm}$;
- d) joining process duration = duration of maintaining at the regime rotation speed = 90 s;
- e) rotation speed: 500 rot/min.

Table 1
Influence of the Joining (Casting) Temperature on the Specific Adherence of the Experimental Bushings for Automobiles

Crt. Nr.	Joining Temp. $T_{\text{mb}}, ^\circ\text{C}$	Detachment resistance, specimens as per fig.4., $A = \text{aria of the surface detached by shearing} = 48 \text{ mm}^2$		
		Applied force F , N	Specific adherence $q = F/A$ N/mm^2	Remarks
1	1020	2880	60	$Q < 70$ soft, non-conform
2	1040	3840	80	$q > 70$ average joint, low
3	1060	5760	120	$70 < q < 170$ average joint, middle
4	1080	7200	150	$70 < q < 170$ average joint, high
5	1100	9600	200	$q > 170$ strong joint
6	1120	9120	190	$q > 170$ strong joint
7	1140	8160	170	$q = 170$ strong joint
8	1160	7200	150	$70 < q < 170$ average joint, high

Metallographic structures of the samples have spotlighted the base material (MB), the deposited layer from the proximity of the joining zone (SD) as well as the interface steel – bronze, joining zone (ZI).

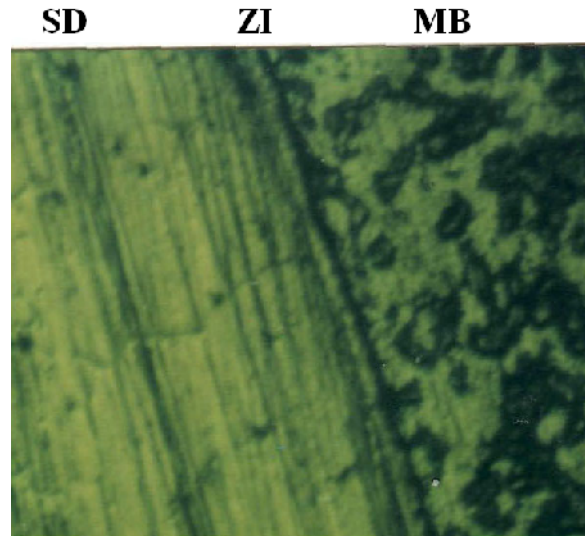


Fig. 5 – Bimetal structure OLT35-CuSn10 ($T_{\text{join.}} = 1,100^{\circ}\text{C}$; $t_{\text{join}} = 120$ s; specific adhesion $q = 200$ N/mm² → hard joint). SD - $\text{ss}\alpha$ polyhedral, MB-ferrite-pearlite structure; ZI-crossing area - dissolved oxides - chemical compounds.

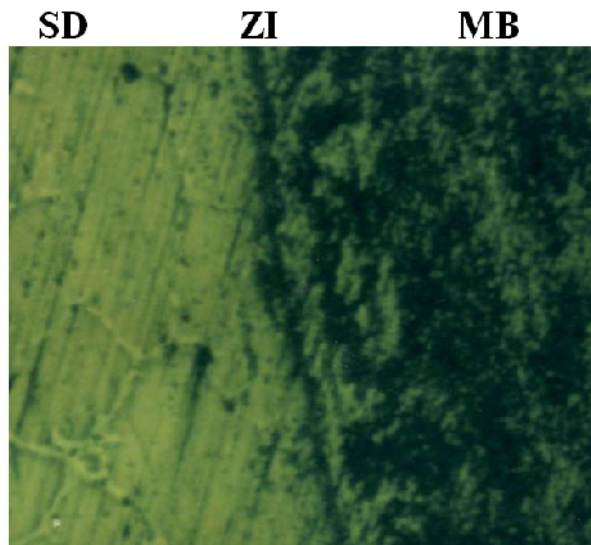


Fig. 6 – Bimetal structure OLT35-CuSn10 ($T_{\text{join.}} = 1,120^{\circ}\text{C}$; $t_{\text{join}} = 140$ s; specific adhesion $q = 190$ N/mm² → hard joint). SD - $\text{ss}\alpha$ polyhedral + acicular inter – metallic compound Cu_3Sn , MB- ferrite + pearlite structure homogeneous, ZI-crossing area - dissolved oxides and small - chemical bonds by diffusion elements.

The non-conform joints have presented the following structure: SD – s.s. α + acicular inter-metallic compound Cu_3Sn ; MB – gross ferrite + perlite; ZI – portions where the partial fusion and the apparition of the joining knots take place; the oxides are maintained in singular places between layers.

The joints with a high specific adherence have presented a structure like this: SD – s.s. α polyhedral; MB – ferite-perlite structure; ZI – passing zone; oxides are dissolved – chemical compounds.

6. Conclusions

1. At joining temperatures $T_{\text{join}} = T_{\text{top1}} + 100$, the specific adherence reaches values $q > 170 \text{ N/mm}^2$ corresponding to the strong joints.

2. At joining temperatures $T_{\text{join}} > T_{\text{top1}} + 100$, the specific adherence decreases towards values of 150 N/mm^2 corresponding to the average joints.

3. Joining temperature does not significantly influence the thickness of the deposited layer.

4. At very high joining temperatures over the optimum determined limit, the joint is no more strong, the resistance of the joint decreases due to the acceleration of the carbon diffusion into the bronze, to the increase of depth of carbon penetration into the bronze, to the high decarburation of the base steel and of the high carburation of the bronze surface, in this way appearing the inter-crystalline corrosion.

REFERENCES

- Corăbieru A., Corăbieru P., *Cilindri bimetalici fabricați prin asamblări ax- tăblie din turnare*. Editura Tehnopress, Iași, 2004, ISBN 973-702-020-0.
- Corăbieru A., Corăbieru P., Velicu S., *Study of the Influence of the Heat Treatments on the Hardness of the Ecological Quaternary Alloys*. Proc. of the 16 th Internat. Conf. on Manufact. Syst. (ICMaS), Published by Edit. Acad. Române, 41-44, București, 2007.
- Corăbieru A., Corăbieru P., C. Predescu, Vasilescu D.D., *Study of the Processing by Heat Treatments of Bimetallic Bushings for Automobiles, of Hypoeutectoid Carbon Steel – Bronze*. The VI-th Internat. Congr. of Mater. Sci. a. Engng., Bul. Inst. Politehnic, Iași, **LIII (LVII)**, 2, s. Materials Science and Engineering, 221 (2007).
- Corăbieru A., Corăbieru P., Vasilescu D.D., *Economic Aspects of the Bimetallic Bushings*. Tehnologia Inovativa, Rev. Construcția de Mașini, 59, 1, 2007, 61.
- Corăbieru P., Corăbieru A., Vasilescu D.D., *Heat Treatments of Bimetallic Bushings*. 3RD Internat. Conf., Adv. Concepts in Mechan. Engng., ACME 2008, Bul. Inst. Politehnic, Iași, **LIV (LVIII)**, 1, s. Construcții de Mașini, 235-240 (2007).
- Corăbieru P., Corăbieru A., Sohaciu M., Vasilescu D.D., *Industrial Applications of the Bimetallic Bushings Economic Aspects*. The VI-th Internat. Congr. of Mater. Sci. a. Engng., Bul. Inst. Politehnic, Iași, **LIII (LVII)**, 2, s. Materials Science and Engineering, 225 (2007).

Velicu S., Zait D., Corăbieru P., Corăbieru A., Vasilescu D.D., *Aspects Regarding the Improvement of the Life Metallic Products Management in the Industry of Auto Components*. Metalurgia Internat., **XIII**, 9, ISI – Edit. Științifică FMR, 2008.

BIMETALE OȚEL – BRONZ OBȚINUTE PRIN IMERSIE ȘI CENTRIFUGARE VERTICALĂ

(Rezumat)

Temperatura de îmbinare este cel mai important factor metalurgic care influențează caracteristicile și structura straturilor bimetalice obținute prin imersie și centrifugare verticală. În scopul de a sublinia influența temperaturii de îmbinare, o serie de parametri au fost menținuți constant și au fost efectuate determinări pentru diferite valori ale temperaturii de îmbinare. Rezultate corespunzătoare au fost obținute la temperaturi cuprinse între $T_{imb.} = 1100^{\circ}\text{C}$ și $T_{imb} = 1160^{\circ}\text{C}$.

BULETINUL INSTITUTULUI POLITEHNIC DIN IAȘI
Publicat de
Universitatea Tehnică „Gheorghe Asachi” din Iași
Tomul LVIII (LXII), Fasc. 2, 2012
Secția
ȘTIINȚA ȘI INGINERIA MATERIALELOR

TRIBOLOGICAL STUDY ON SOME THIN ZINC PHOSPHATE LAYERS

BY

ANDREI VICTOR SANDU*, COSTICĂ BEJINARIU,
IOAN GABRIEL SANDU and CONSTANTIN BACIU

“Gheorghe Asachi” Technical University of Iași
Faculty of Material Science and Engineering

Received: March 5, 2012

Accepted for publication: March 29, 2012

Abstract: The paper presents a tribological study on some thin phosphate layers on iron support. In study were involved friction test, SEM and 3D optical profilometry in order to evaluate the wear resistance and friction coefficient of the obtained layers which have good corrosion resistance.

Keywords: zinc phosphate layers; friction coefficient; SEM; roughness; wear resistance.

1. Introduction

The zinc phosphate layers are commonly used for their protection against corrosion but also as support for paints on steel plates. The layers are obtained by merging or spraying the surfaces with solutions that contains acids and metallic ions. Most of them contain phosphoric acid and zinc and other transitional metals ions (Amirudin & Thierry 1996; Ghali & Potvin 1972; Sandu *et al.*, 2011).

* Corresponding author: *e-mail*: andrew_viktor@yahoo.com

The phosphate coating develops via the nucleation, growth, and coalescence of zinc phosphate grains. The corrosion resistance of the phosphate coating is related to the size and population density of pores in the coating; that is, the pores provide a path for corrosion attack (Bejinariu *et al.*, 2009; Sandu *et al.*, 2010; Zhang *et al.*, 2006).

The article's aim is to characterize the wear resistance and friction coefficient of the obtained zinc phosphate layers deposited on steel.

2. Materials and Methods

The layers were deposited on steel plates (Fig. 1) made of mild steel DC 01 type, (SR EN 10130), used for plastic processing.

Before the obtaining the steel plates were degreased in mild alkaline bath (10 min) followed by pickling in an acid solution (25 min) and then immersion in the phosphate bath.

We selected three types of layers obtained by immersion in the following solutions (composition for one liter):

a) 8.2 mL H_3PO_4 98%, Zn 4g, 2.5 mL HNO_3 60%, 0.7g NaOH, 0.4g NaNO_2 , 0.05g $\text{Na}_3\text{P}_3\text{O}_{10}$ and 12 g $\text{CoCl}_2 \cdot 6\text{H}_2\text{O}$ – **A1**;

b) 8.2 mL H_3PO_4 98%, Zn 4g, 2.5 mL HNO_3 60%, 0.7g NaOH, 0.4g NaNO_2 , 0.05g $\text{Na}_3\text{P}_3\text{O}_{10}$ and 12g $\text{Ni}(\text{NO}_3)_2 \cdot 6\text{H}_2\text{O}$ – **A2**;

c) 8.2 mL H_3PO_4 98%, Zn 4g, 2.5 mL HNO_3 60%, 0.7g NaOH, 0.4g NaNO_2 , 0.05g $\text{Na}_3\text{P}_3\text{O}_{10}$ and 16g $\text{MgS}_2\text{O}_3 \cdot 6\text{H}_2\text{O}$ – **A3**.

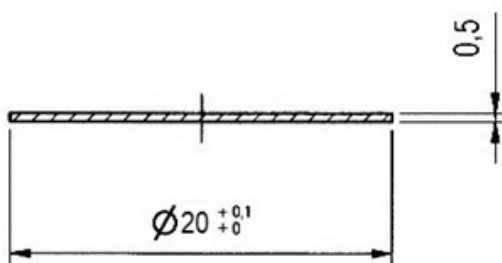


Fig. 1 – The steel plates with the phosphate layers

The tribological test have been carried out with a CSM Tribometer ball on disk type. The samples were placed on the support that is spinning. The range is 5 mm, the speed is 20 cm/s, the applied charge is 2 N and as test head used is a 100C6 steel ball (Ra: 0.02 μm , HRC 62), as in Fig. 2.

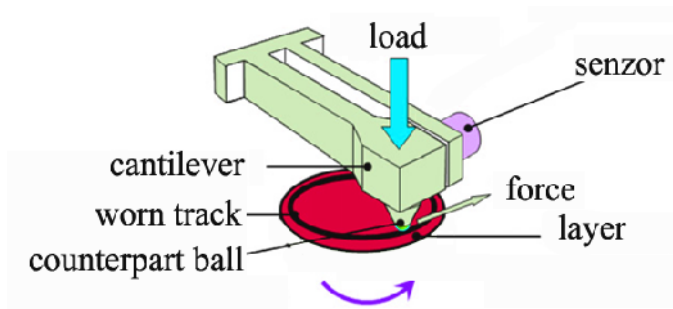


Fig. 2 – The configuration of the tribometer during measuring of the samples.

The microscopic images were obtained with the use of a VEGA II LSH scanning electron microscope manufactured by the TESCAN.

The roughness of the layers was determined with an 3D optical profilometer AltiSurf 500 was used.

3. Results and Discussion

From the Fig. 3 we can observe that the samples had different behaviour on the friction test, **A1** sample presented an increasing of the friction coefficient until it reached 10 m, **A2** at 20 m and **A3** at 26 m. We can consider that the phosphate layers resisted until the lines start descending, being destroyed by the friction with the steel ball.

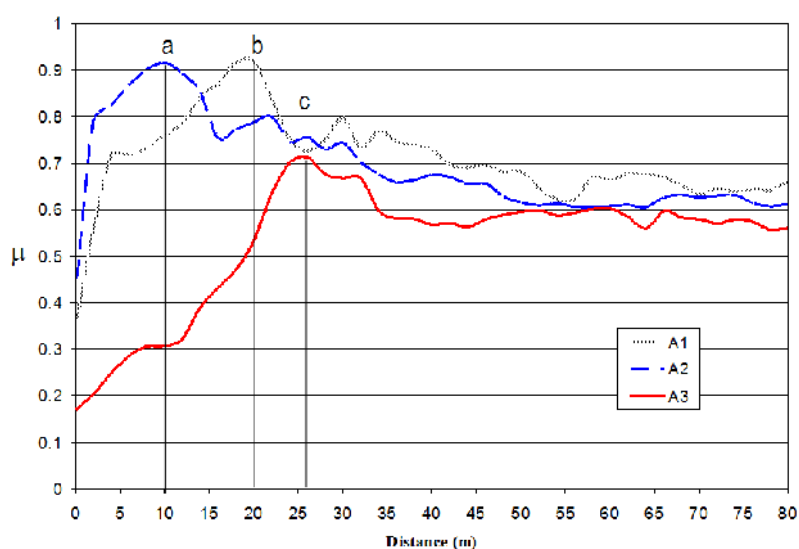


Fig. 3 – Friction coefficient of the samples.

The value of 0.6μ is for the steel plate without any layer on it as seen as average at the end of the graphic.

All the samples were subject to roughness determination, being obtained as average on multiple tests ($n = 8$) on a 5.6 mm line (Table 1).

Table 1
The Roughness of the Samples

Sample	A1	A2	A3
Ra, [μm]	1.9	2.2	1.6

In Fig. 4 we have the SEM images of the phosphate layers.

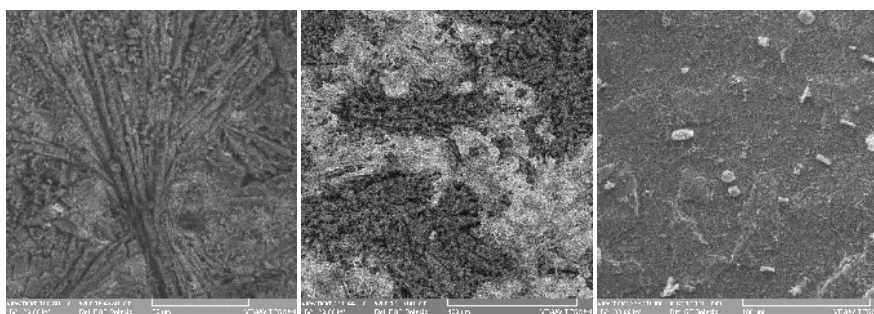


Fig. 4 – SEM images with the samples: A1 – 1500X, A2 – 1000X, A3 – 1000X.

The sample **A1** has a compact layer, this can be seen in the SEM image but also in Fig. 3, where the curve is very smooth, in comparison with **A2** which presents more structures on surface with a higher roughness. **A3** has the lowest roughness and the structure is very uniform.

3. Conclusions

From the roughness and the friction test we can determine that **A3** sample presents the lowest friction coefficient and the highest wear resistance to plastic deformation, this being clear also from the SEM image where the structures are very uniform and homogenous.

The **A1** sample presents a dendrites on surface, and **A2** presents a non-uniform structure, with large particles distributed randomly.

REFERENCES

- Amirudin A., Thierry D., *Corrosion Mechanisms of Phosphated Zinc Layers on Steel as Substrates for Automotive Coatings*. Progress in Organic Coatings, **28**, 59-76, 1996.

- Bejinariu C, Sandu I, Predescu A, Sandu IG, Baciuc C, Sandu AV., *New Mechanisms for Phosphatation of Iron Objects*. Bul. Inst. Politehnic, Iași, s. Știința și Ingineria Materialelor, **LV (LIX)**, 1, 73-77 (2009).
- Ghali E.I., Potvin R.J.A., *The Mechanism of Phosphating of Steel*. Corrosion Science, **12**, 7, 583-594 (1972).
- Sandu A.V., Bejinariu C., Predescu A., Sandu I. G., Baciuc C., Sandu I., *New Mechanisms for Chemical Phosphatation of Iron Objects*. Recent Patents on Corrosion Science, **1**, 1, 33-37 (2011).
- Sandu A.V., Bejinariu C., *Obtaining and Characterization of Superficial Phosphated Layers on Iron Support*. Bul. Inst. Politehnic, Iași, s. Știința și Ingineria Materialelor, **LVI (LX)**, 2, 113-116 (2010).
- Zhang G., Liao H., Li H., Mateus C., Bordes J.-M., Coddet C., *On Dry Sliding Friction and Wear Behaviour of PEEK and PEEK/Sic-Composite Coatings*. Wear 260, 594-600, 2006.

STUDIUL TRIBOLOGIC ASUPRA UNOR
STRATURI SUBȚIRI DE FOSFAȚI DE ZINC

(Rezumat)

Se prezintă studiul tribologic asupra unor straturi subțiri fosfatate pe suport de fier. În studiu s-a apelat la testele de determinare a coeficientului de frecare, microscopia electronică și la profilometria optică 3D în vederea evaluării rezistenței la uzură și a coeficientului de frecare a straturilor obținute ce prezintă rezistența bună la coroziune.

BULETINUL INSTITUTULUI POLITEHNIC DIN IAȘI
Publicat de
Universitatea Tehnică „Gheorghe Asachi” din Iași
Tomul LVIII (LXII), Fasc. 2, 2012
Secția
ȘTIINȚA ȘI INGINERIA MATERIALELOR

REALIZATION OF COMPOSITE HARDENING IN HIGH CARBONACEOUS ALLOYS BY ALLOYING WITH TENSOACTIVE ELEMENTS

BY

V. SAVULIAK*, A. YANCHENKO, A. POSTUPAILO and T. YAROSHENKO

Vinnytsia National Technical University, Ukraine

Received: February 29, 2012

Accepted for publication: March 19, 2012

Abstract: There had been analyzed the influence of surface active elements Va and VIa of subgroups in Mendeleev table on the processes of modification and crystallization of cast iron. It had been demonstrated that liquid cast iron is the single-phase system and represents the carbonic and ferriferous polymer, to the structural base elements of which belong the fullerenes and carbonic nanoparticles on their basis.

Keywords: surface active elements, cast iron modification and crystallisation

Today there are many models for compact (spherical and vermicular) graphitizing, but neither of them can be explain all cases of graphitizing, which occur in practice. This is especially visible during the consideration of anomalous cases of graphitizing in cast irons (without the use of spheroidizing, modifiers, containing sulfur exceeding critical level as well as the effect of overmodification) (Сазонов, 1991; Hughes, 1983).

* Corresponding author: *e-mail*: inmt@inmt.vstu.vinnica.ua

Schools of B. Marynchenko, K. Ortsa and other researches pay much attention to heterogeneous nucleation of graphite in cast on insoluble admixtures. Special attention is paid to the surface active sulphide of the MnS. High dissolubility of FS type sulphide in metal causes the stabilization of cementite by sulfure ions, which are the acceptors of valency electrons (Жуков, 1987).

The activity of insoluble admixtures as substrates depends on their sizes and their tensoactive peculiarities. Papers (Лакедемонский *et al.*, 1960; Лакедемонский *et al.*, 1968) state that high correlation $S/Mn = (0,8-1,2)$ ensures the obtaining of peculiar high –test cast iron with spherical graphite and perlite matrix. Such a structure arises due to the sulfur suppress of the second stage of graphitizing. These cast irons have high strength properties:

$$\sigma_a = 700 - 800 \text{ МПа при } \delta = 6\% .$$

Лакедемонский *et al.*, (1968) and Гиршович (1966) believe that sulfur belong to the elements which hamper graphitizing and impede the isolation of graphite from the smelt, due to the hampering in growth of germ graphite on the stages of screw location.

The main role in the process of graphite germ formation is paid by nonmetallic inclusions (Худокормов, 1968). Their activation takes place in liquid cast iron due to the graphite complexes. The determinant in the activation process is the “adhesion” of foreign particle and graphite complex. Analysing the influential character of different admixture elements on coagulation processes of graphite complexes and conditions of their “adhesion” on non-metallic inclusions, Худокормов, (1968) devides them into graphitizing and non-graphitizing, which is supported by significant experimental material.

According to the researches (Неижко , 1981), the graphite of the spherical form crystallizes when interphase tension and interphase energy of the base edge of graphite in the contact with smelt is smaller than the interphase energy of prismatic edge under simultaneous high surface of cast iron.

During sulfur solution, there arises a significant amount of heat in liquid iron $-\Delta G = -132.1 + 0.0218T$ (Явойский, 1967), which testifies to the appearance of high power connection of the Fe – S type.

During cast iron annealing with $S/Mn \geq 1$, the sulfur to some extend locates in graphite phase, which stipulates for compactness in inclusion of annealing graphite. When $S/Mn \leq 1$ sulfur concentrates basically in sulfide inclusions of MnS type and weakly spherodizes the annealing graphite (Любченко, 1982; Любченко *et al.*, 1968; Любченко *et al.*, 1971). Analogical conclusions may be made from work (Жуков *et al.*, 1981; Жуков *et al.*, 1977). It is possible to point that the possible additional cause for crystallization of graphite on sulfides is the appearance of microcavities on the edges of sulfide-

matrix, as a result of different factors of thermal expansion of sulfides and matrix (Бунин *et al.*, 1967).

Consequently the centers of graphite crystallization may be the microcrystals of lonsdaleite as most profitable substrates both thermodynamically and crystallographically, tensoactive as fo graphite (principle of Dankov) which appear on the initial stage of germ formation.

The process of formation and growth of center of graphite crystallizing on the base of lonsdaleite crystal may consist in the following. The spinoidal exfoliation of high carbonaceous fluctuation on the base of fullerence cluster causes the appearance of drops of “liquid” carbon, in which there takes place the polymerizational structure formation with the creation of nanoparticle. The formation of metallofullerence n the base of iron is probable. In the process of growing of carbonic nanoparticle up to the sizes, ensuring the required level of “buble” pressure, there takes place the reorganization of fullerene structures with the formation of crystal grate of lonsdaleite (Давыдов, 2008).

Fig. 1 shows the microstructure of such cast iron, distinguished by increased content of silicon and sulfur, and the low content of manganese (in % as for the mass: 3.05 C; 2.95 Si; 0,35 Mn; 0.238 S; 0.056 P). The liquid cast iron is processed by 0.01% Bi_2Te_3 . The first stage of annealing is totally complete at 1,223 K in 20 min. The second stage (that is the annealing of ferritic structure) is practically absent – it took place very quickly during cooling process through critical range due to high content of Si in metal.

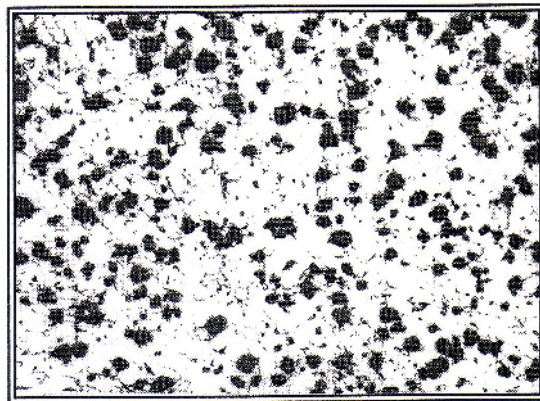


Fig. 1 – Annealed sulphureous high siliceous white cast iron, processed by 0.01% of ligature Bi+Te; thickness of wall of cast assay 40 mm. The thin section is etched by nital. $\times 100$.

Microstructure analysis shows that during the moulding in the dry bar mould the content 3.76% C and 1.48% Si does not allow to receive the perlitic metal base – there is much ferrite in the structure (Fig. 2), however the coils of the same smelt, received from the masslotte moulded in chill contained in their

structure only the low amount of ferrite (Fig. 3). The analogic microstructure was in smelling coils 3 from masslotte, moulded in dry bar mould. The coils of the other groups had pure perlitic structure (Fig. 4).



Fig. 2 – $\times 400$ etching.

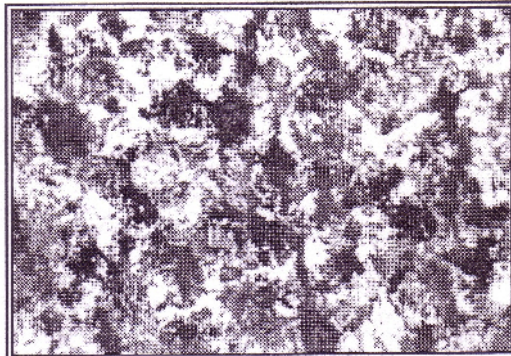


Fig. 3 – $\times 400$ etching.

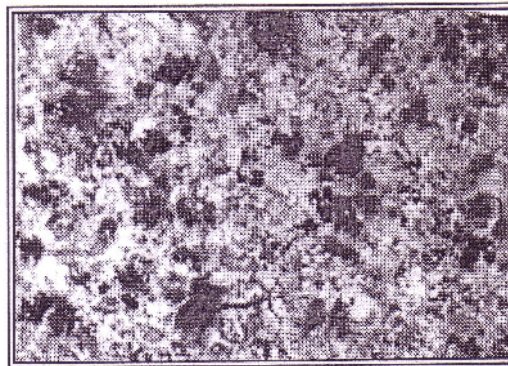


Fig. 4 – Microstructures of experimental smelling, $\times 400$, etching.

Cast iron is high technological metal-carbonaceous alloy, which stipulated for their wide spreading, first of all as a construction material.

Cast iron with fine-grained compact graphite are holding the intermediate position between grey and high-strength cast irons. The assuming technology of their manufacturing is distinguished by stability which practically does not depend on fluctuation of furnace charge content, smelting conditions and other parameters.

Sulfur in most cases not worsen the moulding properties of the new cast irons. It is asserted that the increase of sulfur in cast iron decreases its fluidity and increases tendency to formation of hot cracks. However the decrease in fluidity of usual cast irons takes place due to formation of higher quantity of manganese sulphide in metal. The increase in content of sulfur in low manganese cast irons increases the quantity of eutectic (Давыдов, 2008), decreases eutectic temperature, decreases the tenacity of the melt and, correspondingly improves the fluidity (the sulfur in this case acts as phosphorus analogue).

Inclination of formation of hot cracks in steel and cast iron, which increases together with increase in content of sulfur, is stipulated for by presence of liquid phase in the inter-dendritic sections, which is often preserved up to low temperatures in the result of dendritic segregation.

At the same time the increase in electric with the increased concentration of sulfur in the researched cast irons favours the improvement of continuity which may appear during consolidation of moulding. The sulfide phase is distributed heterogeneously, but not in the form of streaks, and hot-shortness decreases. During cast iron crystallizing there appears the phase with low density-sulphides, which sharply decreases the linear and volume shrinkage.

The determining factor in graphite formation for cast iron of any composition (Жуков *et al.*, 1998; Жуков *et al.*, 2000; Савуляк, 2001), is the excess of sulfur, not connected with manganese, that is the content of free sulfur (ΔS) which is determined by the following formula, but not the correlation S/Mn or Mn/S :

$$\Delta S = [S] - [Mn] / 1.7 . \quad (1)$$

Critical values ΔS , when all graphite is crystallized in compact form, makes up 0.08...0.10%, when the correlation Mn/S fluctuates within 0.75...1.13%.

The high bleaching ability of sulfur (Савуляк, 2002), together with spheroidization of graphite, creates conditions for significant increase in carbon and silicon in the structure of malleablecast iron, without the fear of obtaining the flaked graphite, as well as for speed up in the process of graphitizing annealing. Due to the bleaching influence of sulfur, which increase during the

moulding in the chill mold, it was possible to increase the content of C to 3.5...3.7 %, and Si up to 1.9...2.8%, which ensured the graphitization of cast iron at 1,223 K in 0.5...1.5 h.

The availability of sulphide phase, the sorbitic form of pearlite allowed to use the sulphury cast iron with high anticorrosion and antifricition properties for manufacturing the piston rings (Тодоров, 1974; Жуков *et al.*, 1975). Maslotta, molded from cast iron of the composition 3.4% C, 1.9% Si, $\leq 0.3\%$ Mn, 0.4% S) were annealed during 3 h at 1,253 K, acquiring perlitic structure with equally located inclusions of graphite of compact form (Тодоров, 1974). The high wear resistance of sulphury cast iron is used in manufacturing of finishing instrument (Жуков *et al.*, 1975; Карасева *et al.*, 1978).

It was determined that the sulphide phase co-crystallizes with graphite (Ципунов *et al.*, 1976; Левитин *et al.*, 1981). In cast irons with high content of Mn the sulphide phase is composed of solid solution (Mn Fe) S on the base of compound MnS. In cast irons with low content of Mn was found the complex inclusions of graphite, the central part of which is taken by crystal phase α – FeS. During the slow cooking the sulphide phase is crystallized in the kind of long inclusions of “eutectic deidrids”.

Mechanical properties of the received alloys are presented in table 1. It also includes the copper-oxide cast irons, received by sulfur introduction into metal as ligature Fe – C – Cu – S (Жуков *et al.*, 1998). As is seen from Table 1, in the suggested class of alloys there had been achieved intermediate between the properties of high strength and malleable cast irons on the one hand, and grey cast irons on the other. It should be noted that these new alloys are distinguished by the improved wear resistance, antifricition properties, adjusting and processing by cutting (Давыдов, 2008). They give in to malleable ferritic cast irons in cold tolerance due to the increase in content of silicon.

Foreign countries have recently renewed interest to sulfur as alloying in malleable cast iron (Ципунов *et al.*, 1976; Левитин *et al.*, 1981; Amende, 1978; Меднев *et al.*, 1979). There had been researched the influence of sulfur and manganese on crystallizing and graphitizing of malleable cast iron. With 0.2...0.4% S the process of graphitizing during hardening of cast iron is totally suppressed. In ferritic malleable cast iron it is necessary to restrict the content of S to 0.1% and Mn to 0.55%. The availability of MnS inclusions, which serve as lining for graphite phase of cast iron, favours the cast iron crystallization with non-annealing (Ципунов *et al.*, 1976). In papers (Левитин *et al.*, 1981; Amende, 1978) it is noted that during the introduction of 0.015% Al the compact form of graphite is remained with the excess of S, which equals to 0.25...0.30%. The diffusion of sulfur atoms to the graphite inclusions equals their growth speed in different directions. With the lack of sulfur excess (about 0.1...0.12%), the graphite inclusions due to the increase in growth speed in the direction of decomposition of cementite accept non-regular form.

Table 1
Mechanical Properties of the Received Alloys

% rings	№ melting	Hardness un.HPa	Elasticity,kg	C, %	$\sigma_{\text{bend}} d_H/\text{mm}^2$
1	2c	96, 95, 87	2.3	5.2	48.2
2		95, 93, 97	4.2	7.3	66.5
3		98, 96, 99	4.2	5.6	58.5
4		89, 84, 95	2.5	0.7	29.6
5		93, 86, 89	2.7	0.7	38.4
1	2κ	95, 97, 94	4.5	4.3	85.3
2		97,100, 97	5.0	3.6	64.5
3		96, 97, 96	5.0	4.6	68.7
4		97, 97, 96	5.0	3.7	78.0
5		103,101,99	5.0	5.2	99.1
1	3c	91, 90, 98	4.8	1.0	65.8
2		91, 87, 82	4.5	3.2	66.7
3		89, 89, 89	4.8	3.2	66.7
4		90, 88, 91	5.0	2.8	61.8
5		90, 94, 90	5.0	3.7	76.0
1	3κ	100,94,100	4.4	3.0	110.0
2		92, 100, 97	4.7	5.5	88.5
3		100, 99, 99	5.0	4.8	112.0
4		92, 10, 94	5.0	4.5	87.6
5		99, 100,100	4.6	5.1	75.0
1	4c	99, 97, 98	4.5	6.0	80.0
2		98, 99, 99	4.4	1.2	106.5
3		99, 99, 98	4.8	4.2	80.0
4		97, 97, 99	4.7	3.7	82.0
5		99, 97, 99	5.0	1.1	100.0
1	4κ	99, 99, 97	5.0	2.3	115.2
2		98, 97, 96	5.1	5.6	98.1
3		94, 98, 94	5.1	4.2	83.0
4		93, 96, 98	5.2	3.2	92.0
5		96, 99, 94	5.3	2.4	115.2
1	5c	100,96, 98	5.0	4.2	106.0
2		96, 99, 92	5.0	2.8	108.7
3		102,98, 99	5.0	1.2	112.7
1	5κ	100,101,101	5.3	5.4	115.5
2		101,103,101	5.3	5.4	123.0
3		101,102,101	7.2	5.0	103.0
4		100,102,101	5.3	5.9	122.0
5		99, 102,101	5.0	7.8	122.0
1	6c	97, 96, 97	5.0	6.0	35.0
2		101,101,100	5.0	2.0	122.0
3		98, 99, 99	5.0	3.8	100.2
4		99, 97, 99	5.0	3.5	116.0
1	6κ	97,100,100	5.7	5.7	90.0
2		101,102,102	6.0	3.3	123.0
3		100,102,101	5.7	3.0	127.0

The additive of pirite FeS_2 during the smelting of malleable cast iron ensures the receipt of spheroidizing graphite with the content of S > 0.30% (Amende, 1978).

With the content of sulfur from 0.129% up to 0.533% the cast iron structure changed from ferrite (with 0.128% S) to ferrite-perlite (with 0.233% S), and perlite (with 1.382 and 0.533% S). The stage of spheroidizing of graphite increased along with the growth of redundant content of sulfur. Mechanical properties changed within the following ranges:

$$\sigma_{\hat{a}} = 351 - 501 \text{ MPa}, HB = 1300 - 2340 \text{ MPa}, \delta = 12.8 - 49\%.$$

The bleaching influence of sulfur is very well notice in cast irons. The research of influence of sulfur content from 0.03% up to 0.61% (Давыдов, 2008) on property Ч15 showed that with 0.15% S in the structure there appears the ledeburite cementite, and with 0.3% S there is observed 3...5% of free cementit and interdendrite graphit. The cause for bleaching the authors explain by the appearance tripled light smelting eutectic on the edges of grains, preventing the hydrogen diffusion.

In Меднев it had been stated that with the content of sulfur excess over 0.1% in grey cast iron there appears the interdendrite graphite and grate of carbide on the edges of grains. With the growth of sulfur excess there increases the overcooling of the residual smelt in the interbranches of austenite dendrite and there takes place the crystallization of carbide eutectic.

On the other side, sulfur favours the cast iron graphitizing during the molding. Japan researches state (Дыбенко *et al.*, 1979; Козлов *et al.*, 1974), that during the introduction of carburization into the cast iron prior to output and during the increase in sulfur content in cast iron up to 0.12%, the inclination of such cast iron to bleaching declines considerably. If graphite is introduced prior to cast iron output, the inclination to bleaching does not decrease even with optimal sulfur content, this phenomenon may be explained (Козлов *et al.*, 1974) by decrease in intensivity of graphite particles dilution in the process of their adding to the cast iron with sulfur due to isolation (adsorption) of the sulfur of the graphite surface. In the end the speed of removal of carbon from particles into the smelt decreases and there takes place then stabilization in the dilution processes on pretty low level. During the modifying of grey cast iron (Меднев) by additizings FeSi, FeSiZr, FeSiBa the duration of modifying effect sharply increases with the availability of S up to 0.12% in the smelt, which the authors associate with decontamination in the process of dilution of introduced modifying particles and graphite phase germ due to absorption of sulfur on them. Following the results of (Дыбенко *et al.*, 1979; Козлов *et al.*, 1974; Nobutoro *et al.*, 1979; Nobutoro & Katasumi, 1979) it is possible to conclude that the reason for small sensitivity to modifying FeSi and SiCa of the grey cast iron, smelted on KamAZ (Nobutoro & Katasumi,

1979) lies in the fact that the cast iron is received by the main duplex process: are electric furnace - are electric furnace, which leads to the deep desulfonation of cast iron. In the result during the cast iron modification there is the low resistance of modifying effect due to impossibility of stabilizing particles of temporary fallout graphite by oxygen and sulfur complexes and their quick dilution processes caused by it. The conducted experimental works on researching cast irons with the increase of sulfur content show that the cast iron alloying by sulfur significantly increase the durability and wear resistance of spare parts. In the structure of cast iron with the increased content of sulfur there are inclusions of sulphides of complex structure, which positively influence on its antifriction properties and wear resistance. Apart from that, the factor of dry friction decreases and the speed of running-in increases (Кузнецов & Поручиков, 1979). Under the influence of sulfur the inclusion of carbon annealing are small, numerous and compact. Such a structure favors the retention of oil wedge during liquid friction not worse then in grey cast irons and much better then in high strength and usual malleable cast irons. With such small structure the metal preserves the satisfactory plasticity and viscosity, despite the excessive content of sulphide phase (Жуков *et al.*, 1992).

It had been stated (Жуков *et al.*, 1991) that the mouldings of white cast iron come to the graphitizing annealing with previously developed micro cavities in the form of “cracks” around the sulphide inclusions. The increase in sulfur content causes the increase in number of similar microcavities. The availability of these cavities in inclusions significantly lightens the formation of graphite germs, which in future are the lining for inclusion of carbon annealing.

Considering the scarcity of alloying elements (Cu, Ni, Me, Cr), the availability of significant supply of sulfur in Ukraine, relative simplicity in technology, high content of sulfur in Ukrainian coke, there is a real perspective in development of manufacturing of the new construction material (Шульте, 1976).

Conclusions

Criticism of the “colloidal” theory in structure of liquid cast iron from contemporary positions shows its scantiness and defects. The developed metal and carbon alloys do not differ from traditional alloys through possess the increased micrononhomogeneity. The latter is pretty much stipulated for by the availability in the liquid smelt of the metal and carbon alloys of high carbon clusters, which are formed by polymerization of arena complexes.

Solutions of different polymer forms of carbon in liquid smelt of metal and carbon alloys shall be described by laws of thermodynamics of true nonideal solutions.

Alloying elements and admixtures greatly influence the liquid state of developing metal and carbon alloys. They influence the microheterogeneous composition of smelts and their behavior during consolidation.

Such elements as sulfur, which is surface active as for graphite cluster in melts, influences greatly and forms surface compounds on their base: sulfur as surface- active elements, during specific concentration and conditions favors the compact crystallizing of graphite annealing and favors positively the cast iron matrix, perlitizing it.

REFERENCES

- Сазонов О.А. Синергетическая модель компактной графитизации. Проблемы литейного металлургии чугуна: Межвузовский сборник. Набережные Челны. КамПИ 1991, с. 29-37.
- Hughes I.C.H. The importance and practice of inoculation in iron castings production. In "Solidification Technology in the Foundry and Casthouse". London, Metals society. 1983. p 223-231.
- Жуков А.А. Новое в теории графитизации. Часть 2. – Электронное строение компонентов графитизирующихся систем. Металловедение и термическая обработка металлов. 1987 с 7-14.
- Лакедемонский А.В., Васильев Е.А., Груздов П.Я. Высокопрочный сернистый чугун. – В кн: Передовой научно – технический и производственный опыт: Литейное производство. М: ЦИТЭИ, 1960. вып 6, с 32-38.
- Лакедемонский А.В., Васильев Е.А. Влияние S и Mn на структуру и свойства ковкого чугуна. //Литейное производство. 1968 № 4, с 28-29.
- Гиршович Н.Г. Кристаллизация и свойства чугуна в отливках. М.: Машиностроение 1966, с. 562..
- Худокормов Л.Н. Роль примесей в процессе графитизации чугунов. Минск: Наука и техника. 1968, с.154.
- Неижко И.Г. О роли межфазных границ в формировании графита в чугунах. Новое в металлографии чугуна. Киев: ЧПЛ АН УССР. 1981. с. 11-27.
- Явойский В.И. Теория процессов производства стали. М.: Металлургия 1967, с. 792.
- Любченко А.П. Высокопрочный чугун М.: Металлургия, 1982, с. 120.
- Любченко А.П., Царина И.В., Шерман Л.П. Распределение серы в высокосернистом ковком чугуне.// Литейное производство. 1968, № 7, с. 19-20.
- Любченко А.П., Царина И.В., Шерман Л.П. Микрораспределение серы в ковком сернистых чугунах. //Литейное производство. 1971, № 8, с.21-22.
- Жуков А.А. Карасева В.А. Абаскалов В.Л. Синтез высокосернистых конструкционных чугунов. – В кн: Повышение прочности отливок в машиностроении. М. Наука. 1981, с 79-87.
- Жуков А.А., Бористова О.М., Карасева В.А. Сульфидная фаза в высокосернистых чугунах. //Металловедение и термическая обработка металлов. 1977, № 5, с. 32-35.

- Бунин К.П., Лев И.Е., Репин А.К. Влияние серы и марганца на графитизацию белого чугуна.// Литейное производство. 1967, №12, с.36-38.
- 17.Давыдов С.В. Кристаллизация шаровидного графита в расплаве высокопрочного чугуна // Заготовительные производства в машиностроении, 2008, №3. – с. 3-8.
- Жуков А.А., Савуляк В.И., Пахнющий И.О. Высокосернистые и серно-медистые антифрикционные чугуны улучшенной обрабатываемости резанием. //Металловедение и термическая обработка металлов. 1998. №3, с.3
- Жуков А.А., Савуляк В.И., Архипова Т.Ф. О влиянии элементов на равновесные температуры эвтектических превращений.// Металловедение и термическая обработка металлов. 2000. №2, с.6 .
- Савуляк В.И. Антифрикционная среднеуглеродистая графитизованная сталь. Проблемы трибологии. 2001, №1, с.67-69.
- Савуляк В.И. Синтез зносостійких композиційних матеріалів та поверхневих шарів з екзотермічних компонентів. Вінниця, 2002,160с.
- Тодоров Р.П. Структура и свойства ковкого чугуна. М.:Металлургия. 1974. с.161.
- Жуков А.А., Шалашов В.А., Карасева В.А. и др. - В кн.: Свойства сплавов в отливках. Труды семнадцатого совещания по теории литейных процессов. М.:Наука. 1975. с. 45-49.
- Карасева В.А., Жуков А.А., Ханин Б.Л. и др. Оптимизация химического состава чугуна поршневых колец с повышенным содержанием серы. Литейное производство. 1978. № 11. с.28,29.
- Ципунов В.С., Кронанов В.С., Мазуров И.И. – Заявл. 25.06.74 № 2038618/01. Оpubл. в Б.И., 1976, №26 М И с.22 с.37/00
- А.с. 819204 /СССР/. Чугун/-: Авт. Изоб. В.С. Левитин, Б.Г.Захаров Кропачев, А.П. Пелагейченко. Заявл. 06.10.78 № 2673280/22-02 - Оpubл. в Б.И. 1981. №13, М И с.22 с.37/
- Amende W.Bceinflussen des Gefüges von Temperguß mit Schwefel und Mangan.- Maschinenmarkt. 1978. vol.84. No82 p.1601-1604.
- Меднев А.Е., Стоянов В.И., Мирчева Р.Г. Влияние на модифицирането с акуминий и пито върку количеството и формате на графитните включвания във високосерниста чугуни. - В кн.: Научные труды Высшего института машиностроения, мехнизации и электрификации сельского хозяйства. Русе: 1979, сер.4 №21, с.149-152

REALIZAREA DURIFICĂRII COMPOZITELOR ÎN ALIAJELE BOGATE ÎN CARBON PRIN ALIERE CU ELEMENTE TENSIOACTIVE

(Rezumat)

A fost analizată influența elementelor superficial active din grupa a V-a și a VI-a a tabelului lui Mendeleev asupra procesului de modificare și cristalizare a fontei. S-a demonstrat că fonta lichidă este sistemul monofazic și reprezintă polimerul carbonic și feriferos pentru elementele de bază structurale cărora le aparțin fulerenele și nanoparticulele carbonice ce stau la baza acestora.

